JOURNAL OF VIROLOGY, Dec. 2010, p. 12185–12199 Vol. 84, No. 23
0022-538X/10/$12.00 doi:10.1128/JVI.01447-10

Cell-Cell Spread of Human Immunodeficiency Virus Type 1 Overcomes Tetherin/BST-2-Mediated Restriction in T cells[▽]

Clare Jolly,[1]* Nicola J. Booth,[1] and Stuart J. D. Neil[2]

MRC Centre for Medical Molecular Virology, Division of Infection and Immunity, University College London, London W1T 4JF, United Kingdom,[1] and Department of Infectious Disease, King's College London School of Medicine, Guy's Hospital, London SE1 9RT, United Kingdom[2]

Received 12 July 2010/Accepted 11 September 2010

Direct cell-to-cell spread of human immunodeficiency virus type 1 (HIV-1) between T cells at the virological synapse (VS) is an efficient mechanism of viral dissemination. Tetherin (BST-2/CD317) is an interferon-induced, antiretroviral restriction factor that inhibits nascent cell-free particle release. The HIV-1 Vpu protein antagonizes tetherin activity; however, whether tetherin also restricts cell-cell spread is unclear. We performed quantitative cell-to-cell transfer analysis of wild-type (WT) or Vpu-defective HIV-1 in Jurkat and primary CD4$^+$ T cells, both of which express endogenous levels of tetherin. We found that Vpu-defective HIV-1 appeared to disseminate more efficiently by cell-to-cell contact between Jurkat cells under conditions where tetherin restricted cell-free virion release. In T cells infected with Vpu-defective HIV-1, tetherin was enriched at the VS, and VS formation was increased compared to the WT, correlating with an accumulation of virus envelope proteins on the cell surface. Increasing tetherin expression with type I interferon had only minor effects on cell-to-cell transmission. Furthermore, small interfering RNA (siRNA)-mediated depletion of tetherin decreased VS formation and cell-to-cell transmission of both Vpu-defective and WT HIV-1. Taken together, these data demonstrate that tetherin does not restrict VS-mediated T cell-to-T cell transfer of Vpu-defective HIV-1 and suggest that under some circumstances tetherin might promote cell-to-cell transfer, either by mediating the accumulation of virions on the cell surface or by regulating integrity of the VS. If so, inhibition of tetherin activity by Vpu may balance requirements for efficient cell-free virion production and cell-to-cell transfer of HIV-1 in the face of antiviral immune responses.

Human immunodeficiency virus type 1 can disseminate between and within hosts by cell-free infection or by direct cell-cell spread. Cell-cell spread of HIV-1 between CD4$^+$ T cells is an efficient means of viral dissemination (65) and has been estimated to be several orders of magnitude more rapid than cell-free virus infection (6, 8, 41, 64, 74). Cell-cell transmission of HIV-1 takes place at the virological synapse (VS), a multimolecular structure that forms at the interface between an HIV-1-infected T cell and an uninfected target T cell during intercellular contact (27). Related structures that facilitate cell-cell spread of HIV-1 between dendritic cells and T cells (42) and between macrophages and T cells (16, 17) and for cell-cell spread of the related retrovirus human T-cell leukemia virus type 1 (HTLV-1) (24) have also been described. Moreover, more long-range cell-cell transfer can occur via cellular projections, including filopodia (71) and membrane nanotubes (75). The VS is initiated by binding of the HIV-1 envelope glycoprotein (Env), which is expressed on the surfaces of infected T cells, to HIV-1 entry receptors (CD4 and either CXCR4 or CCR5) present on the target cell membrane (6, 22, 27, 41, 61, 73). Interactions between LFA-1 and ICAM-1 and ICAM-3 further stabilize the conjugate interface and, together with Env receptor binding, help trigger the recruitment of viral proteins, CD4/coreceptor, and integrins to the contact site (27, 28, 61). The enrichment of viral and cellular proteins at the VS is an active process, dependent on cytoskeletal remodeling, and in the infected T cell both the actin and tubulin network regulate polarization of HIV-1 proteins at the cell-cell interface, thus directing HIV-1 assembly and egress toward the engaged target cell (27, 29). Virus is transferred by budding into the synaptic cleft, and virions subsequently attach to the target cell membrane to mediate entry, either by fusion at the plasma membrane or possibly following endocytic uptake (2, 22). In this way, the VS promotes more rapid infection kinetics and may enhance HIV-1 pathogenesis *in vivo*.

Cells have evolved a number of barriers to resist invading microorganisms. One mechanism that appears to be particularly important in counteracting HIV-1 infection is a group of interferon-inducible, innate restriction factors that includes TRIM5α, APOBEC3G, and tetherin (38, 49, 69, 79). Tetherin (BST-2/CD317) is a host protein expressed by many cell types, including CD4$^+$ T cells, that acts at a late stage of the HIV-1 life cycle to trap (or "tether") mature virions at the plasma membranes of virus-producing cells, thereby inhibiting cell-free virus release (49, 56, 81). This antiviral activity of tetherin is not restricted to HIV-1, and tetherin can also inhibit the release of other enveloped viruses from infected cells (31, 40, 54, 62). What the cellular function of tetherin is besides its antiviral activity is unclear, but because expression is upregulated following alpha/beta interferon (IFN-α/β) treatment (1) and tetherin can restrict a range of enveloped viruses, tetherin has been postulated to be a broad-acting mediator of the innate immune defense against enveloped viruses.

* Corresponding author. Mailing address: MRC Centre for Medical Molecular Virology, Division of Infection and Immunity, University College London, Windeyer Building, 46 Cleveland St., London W1T 4JF, United Kingdom. Phone: 44 207 679 9558. Fax: 44 207 679 9555. E-mail: c.jolly@ucl.ac.uk.

▽ Published ahead of print on 22 September 2010.

To circumvent restriction of particle release, HIV-1 encodes the 16-kDa accessory protein Vpu, which antagonizes tetherin and restores normal virus budding (47, 78). The molecular mechanisms by which Vpu does this are not entirely clear, but evidence suggests that Vpu may exert its antagonistic function by downregulating tetherin from the cell surface, trapping it in the trans-Golgi network (10) and targeting it for degradation by the proteasome (12, 39, 81) or lysosome (9, 25, 44); however, degradation of tetherin may be dispensable for Vpu activity (13), and in HIV-1-infected T cells, surface downregulation of tetherin has been reported to be minor (45), suggesting that global removal of tetherin from the plasma membrane may not be necessary to antagonize its function.

Tetherin-mediated restriction of HIV-1 and antagonism by Vpu have been the focus of much research, and inhibition of cell-free virus infection has been well documented (33, 47–49, 77, 81, 82). In contrast, less studied is the impact of tetherin on direct cell-cell dissemination. For example, it is not clear if tetherin-mediated restriction inhibits T cell-T cell spread as efficiently as cell-free release or whether tetherin affects VS formation. To address these questions, we analyzed Vpu^+ and Vpu^- viruses for their ability to spread directly between Jurkat T cells and primary $CD4^+$ T cells in the presence or absence of endogenous tetherin. Our data suggest that tetherin does not restrict HIV-1 in the context of cell-to-cell transmission of virus between T cells expressing endogenous tetherin. Interestingly, we also that observed that Vpu-defective virus may disseminate more efficiently by cell-cell spread at the VS. We postulate that cell-cell spread may favor viral pathogenesis by allowing HIV-1 to disseminate in the presence of tetherin during an interferon-producing innate response.

MATERIALS AND METHODS

Cells, viruses, and tissue culture. The $CD4^+$/$CXCR4^+$ T cell line Jurkat CE6.1 (from the American Type Culture Collection [ATCC]) was maintained in suspension cell growth medium (GM), consisting of RPMI 1640 (Gibco, BRL) supplemented with streptomycin (100 μg/ml), penicillin (100 U/ml), and 10% fetal calf serum (FCS). The HIV-1 clone pNL4.3 and the Vpu-deleted derivative pNL4.3ΔVpu were generously provided by Klaus Strebel (NIAID, NIH) (33). Infectious virus was generated by transfecting plasmids into 293T cells using Fugene 6 (Promega), and virus was harvested after 48 h, quantified by p24 enzyme-linked immunosorbent assay (ELISA) and infectivity assay, and used to infect T cells. To prepare cells infected with HIV-1 wild-type (WT) pNL4.3 or pNL4.3ΔVpu (termed Jurkat-pNL4.3 WT or Jurkat-ΔVpu), 1×10^7 Jurkat cells were infected at an MOI of 0.005 and incubated for 7 to 10 days. Cells were phenotyped for surface Env expression using monoclonal antibody (MAb) 2G12 (Polymun) and for CD4 expression using MAb Q4120 (donated by Q. Sattentau and obtained from the Center for AIDS Reagents [CFAR], National Institutes of Biological Standard and Control [NIBSC], United Kingdom) followed by anti-human or anti-mouse IgG-phycoerythrin (PE) (Jackson Immunoresearch). For conjugate experiments, HIV-1-infected cells were used at 7 to 10 days postinfection, when Env expression was readily detectable and CD4 expression was weak or undetectable. To obtain $CD4^+$ target cells, peripheral blood mononuclear cells (PBMCs) were separated from fresh blood of a healthy HIV-1-seronegative donor using a Ficoll-Hypaque gradient and negatively enriched for $CD4^+$ T cells by magnetic cell sorting according to the manufacturer's instructions (Miltenyi Biotec), and this routinely gave >90% pure $CD4^+$ T cells. Cells were diluted in RPMI 1640–1% FCS (wash buffer [WB]) and used immediately. Alternatively, PBMCs were activated with 1 μg/ml phytohemagglutinin (PHA) (Sigma) and 10 IU interleukin-2 (IL-2) (obtained from the Center for AIDS Reagents, National Institutes of Biological Standard and Control, United Kingdom) for 3 days, and purified $CD4^+$ T cells were infected with pNL4.3 WT or pNL4.3ΔVpu as described above and used as $HIV\text{-}1^+$ donor cells.

Quantification of HIV-1 infection and virus release. Jurkat T cells were infected with pNL4.3 WT or ΔVpu virus, and the percentage of infected cells was quantified by intracellular Gag staining at 2, 4, and 7 days postinfection. Briefly, cells were fixed in 4% formaldehyde, washed, and permeabilized in BD Perm/Wash buffer (BD Biosciences), and HIV-1 Gag was detected with the PE-conjugated antibody RC57-RD1 (Coulter) and data acquired using either a FACSCalibur and CellQuest 5.0 or an LSRII (BD Biosciences) with FACSDiva software. Cell-free supernatants were also collected from HIV-1-infected T cells, and Gag p24 levels were quantified by ELISA as described previously (29). Viral infectivity was measured on HeLa Tzm-bl reporter cells (donated by J. Kappes, X. Wu, and Tranzyme Inc. and obtained from the Center for AIDS Reagents, National Institutes of Biological Standard and Control, United Kingdom) using the Bright-Glo luciferase assay kit (Promega). Viral infectivity was either expressed as 50% tissue culture infective doses ($TCID_{50}$)/ml or normalized to Gag p24 to calculate the $TCID_{50}$/ng p24.

Immunofluorescence (IF) and LCSM. A total of 5×10^5 Jurkat-pNL4.3 WT or Jurkat-ΔVpu cells were washed in WB and incubated on poly-L-lysine (Sigma)-treated coverslips at 37°C for up to 60 min. Cells were then fixed in 4% formaldehyde (FA) in phosphate-buffered saline (PBS)–1% BSA for 15 min at 4°C, followed by quenching in 50 mM ammonium chloride for 10 min at room temperature (RT). For VS experiments, Jurkat-pNL4.3 or Jurkat-pNL4.3ΔVpu cells were mixed with an equal number of primary $CD4^+$ target T cells, and conjugates were allowed to evolve by incubation on poly-L-lysine-treated coverslips for 60 min at 37°C in the presence of the nonblocking MAbs specific for Env (MAb 50-69, donated by S. Zoller-Pazner and obtained from the Center for AIDS Reagents, National Institutes of Biological Standard and Control, United Kingdom) and CD4 (MAb L120.3, donated by D. Buck and obtained from the Center for AIDS Reagents, National Institutes of Biological Standard and Control, United Kingdom) as described previously (27). In some cases a tetherin-specific MAb (Abnova) was included to label surface tetherin at the VS. Alternatively, infected primary $CD4^+$ T cells were used as donor cells and mixed with target cells prelabeled with the CD4 MAb L120. Conjugate evolution was arrested by fixation with cold 4% FA, and the cells were permeabilized in 0.1% Triton X-100–5% FCS for 20 min at RT and washed extensively in PBS. Gag was stained with rabbit antisera against HIV Gag p17 and p24 (donated by G. Reid and obtained from the Center for AIDS Reagents, National Institutes of Biological Standard and Control, United Kingdom) and Vpu with rabbit anti-Vpu (donated by K. Strebel and obtained from the AIDS Research and Reference Reagent Program, Division of AIDS, NIAID, NIH) (37). Primary antibodies were detected with fluorescein isothiocyanate (FITC)-, tetramethyl rhodamine isocyanate (TRITC)-, or Cy5-conjugated donkey anti-mouse, -human, or -rabbit secondary antibodies that were tested for an absence of interspecies reactivity (Jackson Immunoresearch) or with Alexa-conjugated isotype specific anti-IgG1, -IgG2a, or -IgG2b (Invitrogen). Coverslips were mounted with ProLong antifade mounting solution (Molecular Probes), and laser scanning confocal microscopy (LSCM) was performed using a Leica SP2 or SPE laser scanning confocal microscope. Image processing was performed using MetaMorph version 7.1 and Adobe Photoshop version CS2.

Quantification of conjugates and VS. Jurkat-pNL4.3 WT or Jurkat-ΔVpu cells in conjugates with target cells were prepared and analyzed as described above, and multiple random sections of low-power fields were acquired. The total number of effector cells was counted and the percentage of effectors within conjugates quantified. Conjugates were defined as closely apposed pairs of cells containing one $CD4^+$ primary cell and one Env^+ or Gag^+ infected cell. Polysynapses were defined as a single effector cell engaged with multiple target cells. Each conjugate was analyzed for polarization to the cell-cell interface of CD4, Env and Gag, or Vpu and tetherin. Statistical analysis was performed using a nonparametric Mann-Whitney test or analysis of variance (ANOVA) with Bonferroni correction for multiple comparisons. Statistical significance was assumed when the P value was <0.05.

Quantification of cell-cell spread by quantitative real-time PCR and flow cytometry. A total of 5×10^5 Jurkat-pNL4.3 WT or Jurkat-ΔVpu cells were mixed with an equal number of uninfected T cells and incubated for up to 6 h. At 0, 1, 3, and 6 h postmixing, cells were lysed, genomic DNA was extracted (Qiagen), and quantitative real-time PCR was performed using an ABI 7000 to measure cell-cell spread of HIV-1 (29). Alternatively, pNL4.3 WT- or ΔVpu-infected primary T cells were mixed with uninfected T cells for 0, 3, 6, or 12 h and analyzed by real-time PCR. In some cases, target cells were pretreated with 10 μM zidovudine (obtained from the NIH AIDS Research and Reference Reagent Program) for an hour at 37°C to achieve a final concentration of 5 μM after donor and target cells were mixed. To measure cell-cell spread by flow cytometry, an adaptation of the assay of Sourisseau et al. (74) was used. Briefly, an equal number of HIV-1-infected donor cells were mixed with carboxyfluorescein succinimidyl ester (CFSE) or CellTrace Far Red-labeled target T cells (2 μM; Invitrogen) and incubated for 0, 6, and 24 h at 37°C. In some cases, target cells

were pretreated with 10 μM zidovudine as described above. Cells were then fixed in 4% formaldehyde, washed, and permeabilized in BD Perm/Wash buffer (BD Biosciences), and HIV-1 Gag was detected with the PE-conjugated antibody RC57-RD1 (Coulter) and data acquired using either a FACSCalibur and CellQuest 5.0 or an LSRII (BD Biosciences) with FACSDiva software. Flow cytometry acquisition for gating on single cells was performed on the LSRII using doublet discrimination. The percentage of Gag^+ CFSE or CellTrace $FarRed^+$ labeled target cells was quantified and data analysis performed using CellQuest 5.0 or FlowJo.

Interferon induction of tetherin expression. Jurkat-pNL4.3 WT, Jurkat-pNL4.3ΔVpu, or infected primary $CD4^+$ T cells were treated with 500 U/ml of IFN-β (a kind gift from M. Noursadeghi, UCL) for 24 h prior to being mixed with target cells and analyzed by LSCM and real-time PCR. Uninfected Jurkat T cells and primary $CD4^+$ T cells were similarly treated with IFN-β; surface stained for tetherin, LFA-1 (MAb L130; BD Biosciences), and ICAM-1 (MAb LB-2; BD Biosciences); and analyzed by flow cytometry.

RNA interference (RNAi) knockdown of tetherin. At total of 1×10^6 Jurkat T cells or primary $CD4^+$ T cells were nucleofected (Amaxa) with either small interfering RNA (siRNA) oligonucleotides targeting tetherin or control sequences (Dharmacon Smartpool catalogue numbers L-011817 and D-001210-01-20, respectively), and 24 h later cells were infected with pNL4.3 WT or pNL4.3ΔVpu virus at an MOI of 0.05. After 72 h, the infected cells were mixed with uninfected T cells, cell-cell spread was measured by real-time PCR, and VS formation was quantified. Knockdown of tetherin expression was confirmed by surface staining and flow cytometric analysis.

SDS-PAGE and Western blotting. Jurkat-pNL4.3 WT or Jurkat-pNL4.3ΔVpu cells were pelleted by centrifugation, and cells were washed twice in cold PBS. Cell pellets were lysed (radioimmunoprecipitation assay [RIPA] buffer, consisting of 50 mM Tris-HCl [pH 8], 150 mM NaCl, 1% NP-40, 0.1% SDS, 0.5% deoxycholic acid, 1 mM phenylmethylsulfonyl fluoride [PMSF], and Complete protease inhibitor Cocktail [Roche, United Kingdom]) on ice for 10 min, and soluble protein collected following centrifugation at $15{,}000 \times g$ for 10 min at 4°C. Lysates were stored at −80°C, and the protein concentrations were determined using a bicinchoninic acid (BCA) protein assay reagent kit (Pierce). Virus was purified from cell-free supernatants by ultracentrifugation through a 25% sucrose cushion, and pelleted virus was resuspended in equal volumes of PBS and stored at −80°C. Twenty micrograms of cell lysate and an equal volume of purified virus were separated by SDS-PAGE. Proteins were transferred onto nitrocellulose, blocked in PBS with 0.5% Tween 20 and 5% skim milk (Marvel), probed with rabbit antiserum raised against HIV-1 Gag (donated by G. Reid and obtained from the CFAR) or actin (Sigma) followed by goat anti-rabbit–horseradish peroxidase (HRP) (Dako), and visualized by enhanced chemiluminescence (ECL) (Amersham).

TEM. Jurkat T cells were infected with pNL4.3 or Jurkat-pNL4.3ΔVpu and cultured for 10 days before being prepared for transmission electron microscopy (TEM) as described previously (27). Briefly, the cells were pelleted by centrifugation, fixed in 0.5% glutaraldehyde, and postfixed in 1% osmium tetrozide and 1.5% potassium ferricyanide for 1 h. After extensive washing in water, the cells were incubated in 0.5% magnesium uranyl acetate, dehydrated, and embedded in Epon resin. Ultrathin sections were cut, collected on TEM grids, and stained with lead citrate. Sections were analyzed using a Philips FEI Technai 12 transmission electron microscope, and digital images were captured using Soft Imaging software and processed using Abode Photoshop.

RESULTS

Vpu-deficient HIV-1 disseminates efficiently between $CD4^+$ T cells. In order to investigate the effect of Vpu on cell-cell spread of HIV-1, 293T cells were transfected with plasmids encoding either full-length pNL4.3 wild-type virus or pNL4.3 with a defective Vpu gene (ΔVpu) to generate infectious HIV-1 pNL4.3 WT and pNL4.3ΔVpu virus (33, 77). To confirm that these viruses displayed the appropriate Vpu-dependent cell-free budding defect, Jurkat T cells were infected with HIV-1 pNL4.3 WT or pNL4.3ΔVpu, and cell-free virus release from T cells was examined by Western blotting at 72 h postinfection (Fig. 1A) and infected cells visualized by electron microscopy (Fig. 1B). In agreement with previous reports, T cells infected with the Vpu-defective virus pNL4.3ΔVpu released less Gag p24 than those infected with pNL4.3 WT, with a concomitant increase in cell-associated p24 (Fig. 1A) (33, 47, 49, 81). Electron microscopy imaging confirmed that nascent pNL4.3ΔVpu virions were retained at the plasma membrane by characteristic membrane tethers (Fig. 1B) (49).

To examine cell-cell spread of HIV-1 between T cells in the presence and absence of Vpu (and, by extension, antagonized and unantagonized tetherin), Jurkat T cells were infected with either pNL4.3 WT or pNL4.3ΔVpu at a low MOI of 0.005 to favor cell-cell spread, and at various time points thereafter virus release was quantified by infectivity assay and infected cells enumerated by intracellular Gag staining and flow cytometry (Fig. 1C). As expected, more infectious virus was present in supernatants harvested from cells infected with pNL4.3 WT virus than in those from cells infected with pNL4.3ΔVpu at 2 days postinfection (Fig. 1C), when there were equivalent numbers of Gag^+ cells, likely reflecting more efficient cell-free particle release, in agreement with Fig. 1A. Interestingly, this effect was not apparent at later time points (days 4, 7, and 10 postinfection [$P > 0.05$]) and appeared to correlate with an increase in the percentage of Gag^+ T cells in the ΔVpu-infected cultures compared to WT-infected cultures. Notably, pNL4.3 WT and pNL4.3ΔVpu viruses produced by infected Jurkat cells showed the same relative infectivity when normalized to Gag p24 (Fig. 1D), demonstrating that the difference in replication kinetics is not due to pNL4.3ΔVpu virus being inherently more infectious than WT virus and suggesting that Vpu-defective HIV-1 may disseminate efficiently by direct T cell-T cell transmission.

To rule out that doublets or aggregates between infected and uninfected cells may be artificially increasing the detection of Gag^+ cells, additional experiments were performed on Jurkat cells infected with pNL4.3 WT or pNL4.3ΔVpu, in which we gated on the total live cell population and additionally gated out only the single cells using doublet discrimination. Figure 1E shows that most of the cells in the infected cell population were indeed single cells, with relatively few cells apparent outside the single cell gate and no clear doublet population (which would appear as a distinct population below the single cells). There was no difference in intracellular Gag staining between the total cell population and the single-cell group, demonstrating that doublets or aggregates between infected and uninfected cells are infrequent and do not artificially increase our detection of Gag^+ infected cells. In addition, infected cells were treated with trypsin-EDTA prior to fixing to further diminish doublet formation and to remove surface-absorbed p24. There was no difference in the intracellular Gag staining between cells treated with trypsin-EDTA and those left untreated (Fig. 1E), providing further evidence that doublets are infrequent and indicating that most of the Gag p24 that we are detecting by flow cytometry is likely to be intracellular.

Quantification of VS formation by WT and Vpu-defective HIV-1. Cell-cell spread of HIV-1 takes place at virological synapses. To investigate the effect of Vpu and tetherin on VS formation, Jurkat T cells were infected with either pNL4.3 WT (termed Jurkat-pNL4.3 WT cells) or pNL4.3ΔVpu (Jurkat-ΔVpu cells), mixed with primary $CD4^+$ target T cells, and examined for virological synapse (VS) formation by immunofluorescence labeling (IF) and laser scanning confocal microscopy (LSCM) (Fig. 2A). The T cell VS is characterized by

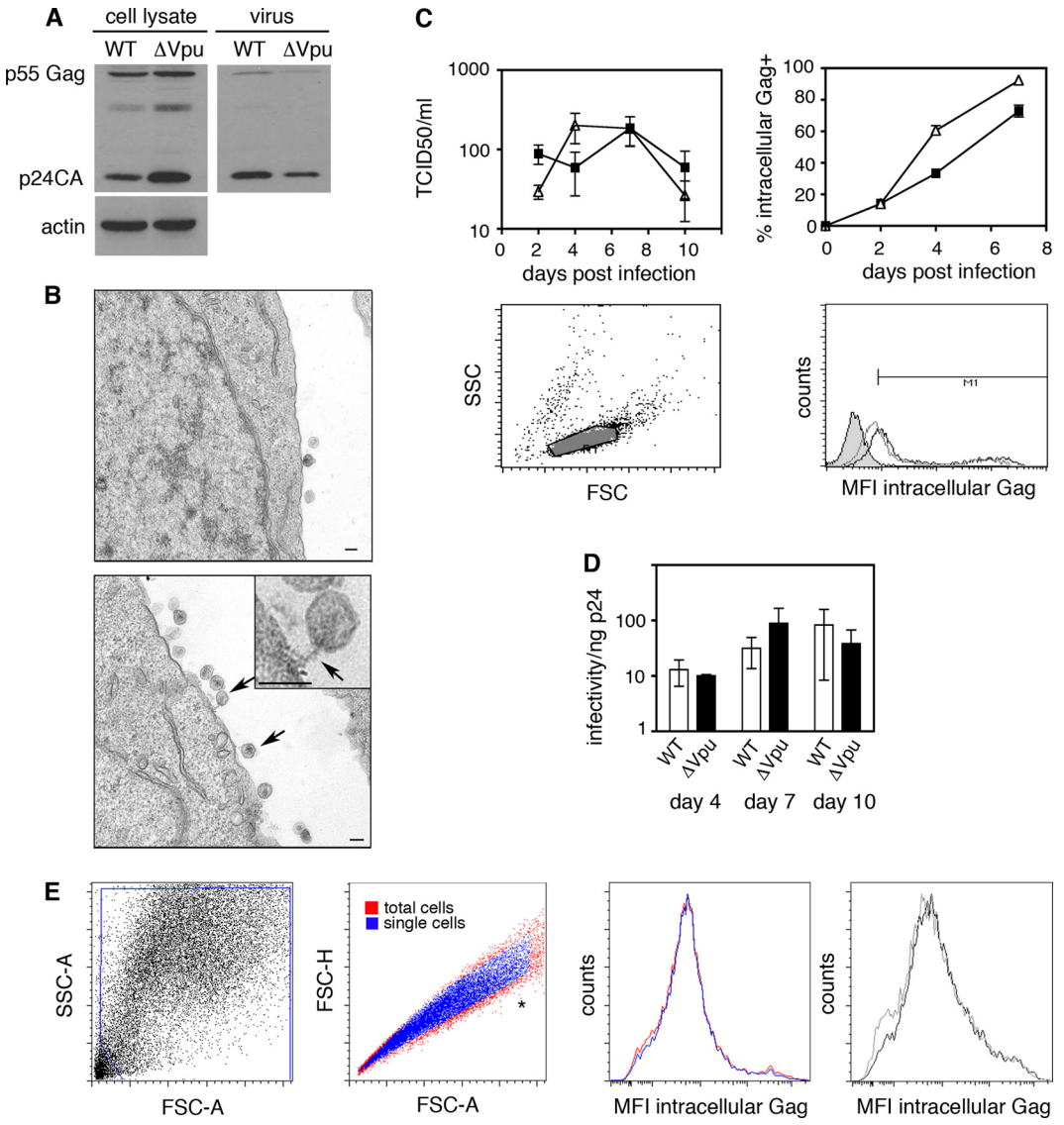

FIG. 1. Confirmation of the Vpu-mediated budding defect in Jurkat T cells. (A) Jurkat T cells were infected with pNL4.3ΔVpu or pNL4.3 WT virus, and at 3 days postinfection the cells were pelleted and virus-containing supernatants were harvested and purified by ultracentrifugation. Equal volumes of virus particles and concentrations of cell lysates were analyzed by SDS-PAGE and Western blotting using rabbit antiserum against HIV-1 Gag and an anti-actin loading control. (B) Jurkat T cells were infected with either pNL4.3 WT or pNL4.3ΔVpu, fixed and processed for TEM. Ultrathin sections of infected cells show more virions accumulating on the plasma membrane of cells infected with ΔVpu virus (lower panel) than on that of cells infected with Vpu-expressing, wild-type virus (upper panel). Virions tethered to the plasma membrane are characteristic of Vpu-defective virions and are indicated with arrows. The boxed region shows a tethered virus at a higher magnification. Scale bar, 100 nm. (C) Vpu-defective virus disseminates efficiently in culture. Jurkat T cells were infected with either pNL4.3ΔVpu (triangles) or pNL4.3 WT (squares). The amount of infectious virus in the supernatants was quantified by luciferase assay using HeLa Tzm-bl reporter cells (expressed as $TCID_{50}$/ml) (upper left panel), and the percentage of infected Jurkat cells was quantified by intracellular Gag staining and flow cytometry (upper right panel). Data are from the identical experiments and are the means from three independent experiments; error bars show the SEMs. The lower left panel shows a representative example of gating on the live cell population using FACSCalibur and CellQuest 5.0, and the histogram (lower right panel) shows the intracellular staining of cells infected with either WT (gray line) or ΔVpu (black line) virus at 7 days postinfection overlaid onto stained, uninfected control cells (gray filled). The M1 marker was set to the position that excluded >99% of the uninfected cells to define the Gag-positive population. Results from a representative experiment are shown. (D) pNL4.3 WT and pNL4.3ΔVpu viruses have the same relative infectivity. Cell-free supernatants were harvested at various times postinfection and quantified for viral infectivity by luciferase assay. Data are shown as the $TCID_{50}$ per ng of p24 to normalize for any differences in the viral content of supernatants. Data are from four independent experiments, and error bars show the SEMs. (E) Comparison of intracellular Gag staining with total-cell and single-cell gating. Jurkat cells infected with either WT or ΔVpu virus were fixed and stained for intracellular Gag, and data were acquired using an LSRII flow cytometer and FACSDiva software. The first gate was applied to define the total cell population (far left panel), and this population was then analyzed using FSC-A versus FSC-H for doublet discrimination (middle left panel), with a second gate applied to differentiate single cells (blue) from the total population (red) to exclude doublets. Note that there are few cells in the position expected for the doublet population (denoted with an asterisk). The histogram (middle right) shows an overlay of intracellular Gag staining of the total cell population (red line) compared to single cells (blue line). The far right panel shows an overlay of intracellular Gag staining of infected cells either left untreated (black line) or pretreated with trypsin-EDTA prior to fixing (gray line). Results from a representative experiment are shown, and similar results were seen with both WT and ΔVpu viruses.

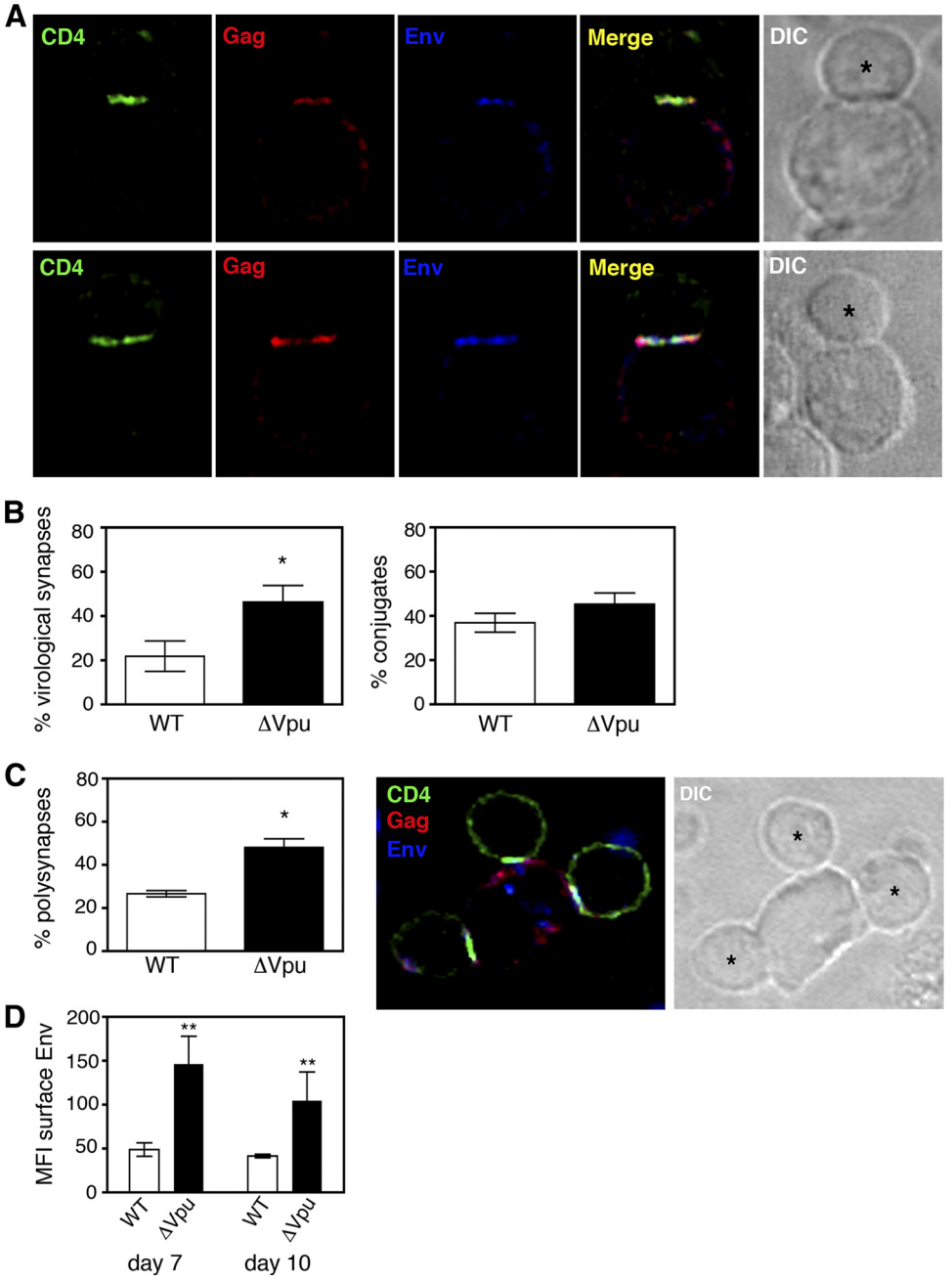

FIG. 2. ΔVpu virus induces VS formation more efficiently than WT Vpu-expressing virus. (A) HIV-1-infected cells were mixed with uninfected primary target T cells (asterisks) in the presence of nonblocking MAbs against Env (blue) and CD4 (green) and incubated for an hour at 37°C. Conjugates were fixed, permeabilized, stained for Gag using rabbit antiserum (red), and analyzed by LSCM. Areas of colocalization appear yellow. VSs between target cells and Jurkat-pNL4.3 WT (upper panel) or Jurkat-ΔVpu (lower panel) cells show similar copolarization of CD4 and Env/Gag to the cell-cell interface. (B) Quantification of conjugate and VS formation between HIV-1 infected T cells and target T cells. Jurkat-pNL4.3 WT (white bars; $n = 183$) and Jurkat-ΔVpu (black bars; $n = 231$) cells were mixed with target cells, stained, and scored for whether or not they had formed a conjugate with a primary T cell (defined as closely apposed pairs consisting of a single target cell and a single effector cell, excluding polysynapses) and whether the conjugate had evolved a VS (Jurkat-pNL4.3 WT, $n = 65$; Jurkat-ΔVpu, $n = 117$). Data are from three independent experiments, and error bars show the SEMs. (C) Quantification of the frequency of polysynapse formation between Jurkat-pNL4.3 WT cells (white bars; $n = 45$) or Jurkat-ΔVpu cells (black bars; $n = 108$) and target cells. Polysynapses were defined as a single effector cell engaging multiple target cells, and a representative polysynapse between a Jurkat-ΔVpu cell and a target T cell is shown. Data are from three independent experiments, and error bars show SEMs. (D) Jurkat-ΔVpu cells express more HIV-1 envelope glycoprotein (Env) at the cell surface. Jurkat-pNL4.3 WT (white bars) and Jurkat-ΔVpu (black bars) cells were surface stained for HIV-1 Env with MAb 2G12 on days 7 and 10 postinfection and analyzed by flow cytometry by gating on the live cells. Env-positive staining was defined by comparison with control stained cells (infected cells stained with secondary antibody only) and was set at the MFI that excluded >99% of the control cells (see Fig. 1); from this the MFI of the Env-positive population was determined. Data are means and SEMs from seven independent experiments. *, $P = <0.05$; **, $P = <0.01$; ***, $P = <0.005$; ****, $P = <0.001$.

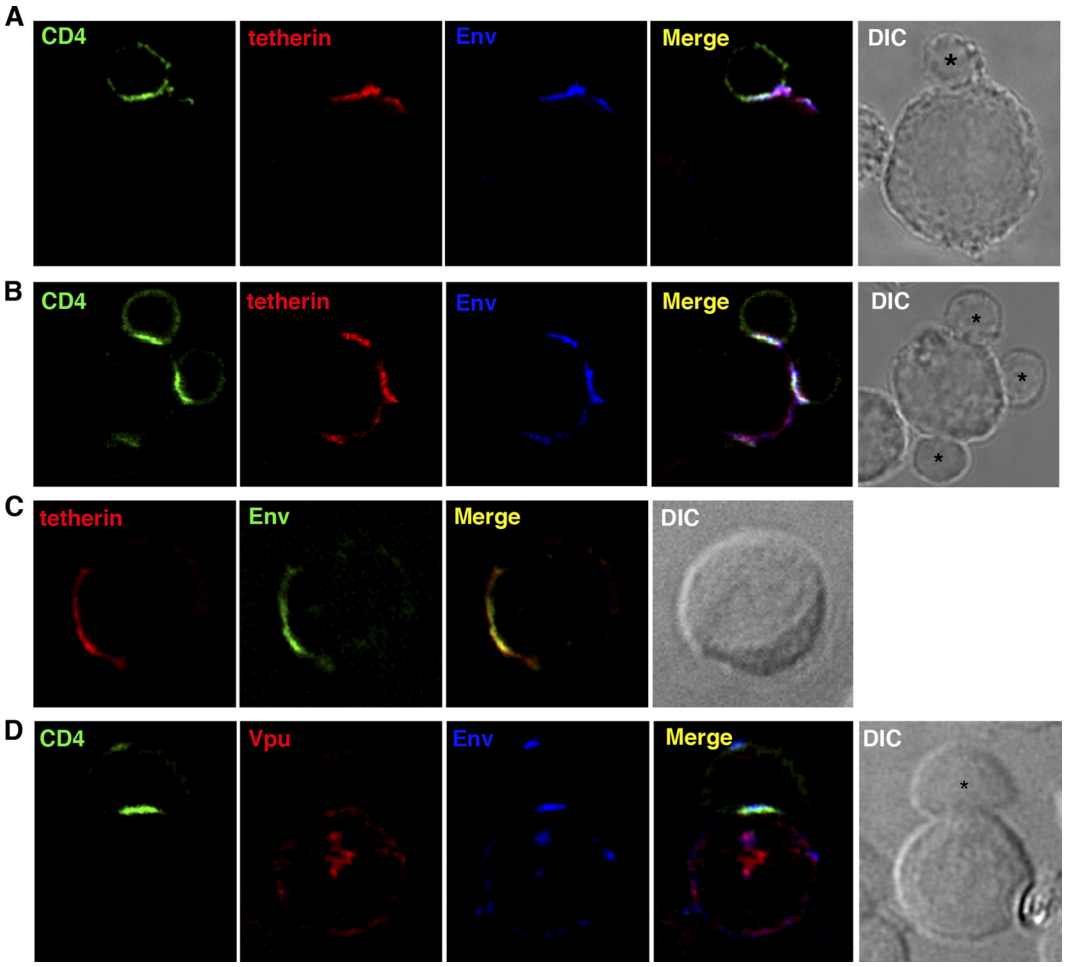

FIG. 3. Tetherin but not Vpu colocalizes with Env at the VS. (A) Jurkat-ΔVpu cells were mixed with uninfected target T cells and incubated for an hour at 37°C in the presence of MAbs against Env (blue), CD4 (green), and tetherin (red) in order to stain surface proteins. Endogenous, surface-expressed tetherin is enriched on the HIV-1-infected T cell at the VS and colocalizes with Env ($n = 64$). The target cell is indicated with an asterisk. (B) Tetherin is enriched at multiple contact sites on polysynapses. Env, blue; CD4, green; tetherin, red. (C) Tetherin colocalizes with HIV-1 Env on infected T cells not engaged in a VS. Jurkat-ΔVpu cells were surface stained for Env (green) and tetherin (red) in the absence of target T cells. (D) Jurkat-ΔVpu cells were mixed with uninfected target T cells and incubated for an hour at 37°C in the presence of MAbs against Env (blue) and anti-CD4 (green). Cells were fixed, permeabilized, and stained for intracellular Vpu (red). Vpu localized mainly in the perinuclear region and was not enriched at the VS ($n = 26$).

coenrichment of HIV-1 Env and Gag on the infected cell and of CD4 on the target cell at sites of cell-cell contact (27). Quantification of conjugate and VS formation revealed that Jurkat-ΔVpu cells were not impaired in VS formation but, interestingly, formed significantly more synapses than Jurkat-pNL4.3 WT cells (46% and 22%, respectively; $P = 0.03$), and this was not due to enhanced conjugate formation (37% and 45%, respectively; $P = 0.2$) (Fig. 2B). In addition, VSs that formed between Jurkat-ΔVpu cells and target T cells were morphologically similar to those for Jurkat-pNL4.3 WT cells in recruitment of CD4, Env, and Gag (Fig. 2A). Moreover, we also detected more polysynapses forming between target T cells and Jurkat-ΔVpu cells (defined as a single HIV-1-infected cell interacting with >1 target cell with clustering of HIV-1 at multiple sites of cell-cell contact [61]) than with Jurkat-pNL4.3 WT cells (48% and 26%, respectively; $P = 0.02$) (Fig. 2C).

To address the apparent increase in VS formation in the absence of Vpu, flow cytometry was performed to measure HIV-1 Env surface expression. These analyses revealed that Jurkat-ΔVpu cells express up to 3-fold more envelope glycoprotein at the cell surface than Jurkat-pNL4.3 WT cells ($P = 0.008$) (Fig. 2D). Because unantagonized tetherin physically retains Env-expressing virions at the cell surface, this result is not entirely unexpected; however, since Env-receptor interactions are known to drive VS formation (27), increased exposure of Env at the plasma membrane may contribute to the increased frequency of VS formation by Vpu-defective HIV-1.

Tetherin, but not Vpu, is a component of the VS. Next we investigated whether tetherin was present at sites of cell-cell contact. To do this, conjugates between Jurkat-ΔVpu and target T cells were allowed to form in the presence of monoclonal antibody to label cell surface tetherin and then fixed, stained, and analyzed by confocal microscopy. We detected copolarization of tetherin with Env on infected T cells at sites of cell-cell contact in the majority of VSs examined (65% $n = 64$) (Fig. 3A), and tetherin also localized at multiple sites of cell-cell

contact seen during polysynapse formation (Fig. 3B). Strong enrichment of tetherin at the VS was often associated with strong Env polarization (data not shown). Moreover, tetherin could sometimes be visualized on the target T cell at the cell-cell interface, possibly due to incorporation into transmitted virions attached to the target cell membrane (56). Tetherin also colocalized with Env on the surface of unconjugated HIV-1-infected T cells (Fig. 3C) that were not engaged in a VS (75% ± 6% [mean ± standard error of the mean {SEM}]; $n = 55$), indicating that tetherin is a component of sites of HIV-1 assembly and budding of cell-free virus. Collectively, these data show that tetherin is present in the VS but that it does not impair cell-cell contact or VS formation.

To investigate whether Vpu was similarly enriched at the VS in Jurkat-pNL4.3 WT cells, conjugates were permeabilized and stained for Vpu. Intracellular Vpu was clearly visible in HIV-1-infected cells and was often localized to perinuclear regions, as described previously (33). Unlike tetherin, Vpu was only infrequently associated with the VS (14%; $n = 26$) and did not appear to be enriched at sites of cell-cell contact (Fig. 3D). Thus, recruitment of Vpu to the VS does not appear to be essential for VS formation and cell-cell spread.

Quantification of cell-cell spread by WT and Vpu-defective HIV-1. To directly compare the efficiencies of cell-cell transfer in the presence and absence of Vpu and thus endogenous tetherin, we performed a flow cytometry assay to quantify the appearance of Gag^+ target T cells following coculture with pNL4.3 WT- or pNL4.3ΔVpu-infected T cells (74). Dye-labeled target T cells were incubated with WT- or ΔVpu-infected T cells at 7 to 10 days postinfection (both routinely were >80% infected [data not shown]) for 6 h and 24 h, fixed, permeabilized, and stained for intracellular Gag, and the number of Gag^+ dye-labeled target cells was quantified by flow cytometry (Fig. 4A). Gag transfer from both WT- and ΔVpu-infected cells to dye-labeled target cells was detected within 6 h of coculture, increasing approximately 3-fold by 24 h. This is a time frame in which dissemination of virus is by direct cell-cell rather cell-free transfer due to faster transmission kinetics of cell-cell dissemination (6, 8, 29, 41, 74). Figure 4A shows that both WT and ΔVpu viruses were capable of disseminating between T cells, as evidenced by the appearance of the Gag^+ dye-labeled population, and that cell-cell transfer of Vpu-defective HIV-1 from tetherin-expressing T cells was not impaired compared to that of WT virus. In fact, cell-cell transfer of ΔVpu virus appeared to be somewhat more efficient than that of WT virus at both 6 h (12.5% and 3.1%, respectively; $P < 0.001$) and 24 h (36.7% and 14%, respectively; $P < 0.001$). To check that the appearance of Gag^+ target cells was not a result of formation of doublets between infected and uninfected cells rather than *bone fide* acquisition of Gag through virus transfer, we repeated the experiment and performed additional analysis to exclude doublets by gating out single cells from the total live cell population, an example of which is shown in Fig. 4B. We found little difference in the number of Gag^+ target cells detected when applying either gating strategy, confirming that this assay is appropriately detecting cell-cell transfer of both WT and ΔVpu viruses. The lack of a detectable population of doublets is in agreement with estimates that the average life span of the T cell VS is roughly 1 h, after which >90% of conjugates separate (41). In addition, treating cells with trypsin-EDTA after coincubation but prior to fixing had no effect on the proportion of Gag^+ target cells detected after 6 h (data not shown), in agreement with Fig. 1E, suggesting that most of the Gag staining that we detected is intracellular.

To investigate whether the intracellular Gag that we detected in target T cells is due to the synthesis of new Gag protein as a result of productive infection, target T cells were either left untreated or treated with the reverse transcriptase inhibitor zidovudine prior to being mixed with donor cells (Fig. 4C). Inhibition of reverse transcription had no effect on the mean fluorescence intensity (MFI) of Gag staining in the newly infected Gag^+ target cell population after only 6 h of coculture, as expected, because within this short time period we will be detecting mostly transfer of viral material rather than new Gag synthesis. In contrast, after 24 h of incubation, target cells treated with zidovudine showed a partial reduction in the MFI of Gag staining following coculture with WT- or ΔVpu-infected cells, demonstrating that some of the Gag signal detected in newly infected target cells does indeed result from *de novo* synthesis as a result of productive infection. The accumulation of Gag in both zidovudine-treated and untreated target cells after 24 h likely represents the continual and nonreversible transfer of virus during coculture.

To follow cell-cell transfer using a different assay system we used a quantitative real-time PCR assay that measures *de novo* synthesis of HIV-1 *pol* DNA transcripts as a marker of new virus infection (29, 41). This assay detects late HIV-1 reverse transcripts that are relevant to postentry infection events and proximal to integration and productive infection, and treating target T cells with zidovudine appropriately reduces the detection of RT products (Fig. 4D). Jurkat-pNL4.3 WT- and Jurkat-ΔVpu-infected cells were mixed with target T cells and incubated for 1, 3, and 6 h at 37°C, and real-time PCR was performed (Fig. 4D). This is a time frame that allows detection of *pol* reverse transcript products arising from efficient cell-cell spread but not cell-free infection (29, 41, 74). In support of the results obtained when quantifying cell-cell spread by flow cytometry, Fig. 4D reveals that after 6 h of coculture between pNL4.3-Vpu infected cells and target cells, a 6-fold increase in the appearance of reverse transcripts over the baseline level ($t = 0$ h) was detected, indicative of cell-cell spread. In contrast, WT virus appeared to be less efficient and displayed a more modest 1.2-fold increase ($P < 0.05$), again suggesting more rapid dissemination of Vpu-defective HIV-1.

Interferon treatment of T cells upregulates tetherin expression and inhibits virus release in the absence of Vpu (48, 49). To examine the effect of tetherin upregulation in the context of cell-cell spread at the VS, Jurkat-pNL4.3 WT and Jurkat-ΔVpu cells were pretreated with IFN-β for 24 h, washed, and assayed for cell-cell spread by flow cytometry and real-time PCR (Fig. 4A and D). Notably, although the release of nascent cell-free virus was impaired after IFN treatment (Fig. 4E) and tetherin surface expression was upregulated (Fig. 4F), confirming appropriate activity of this cytokine, IFN treatment and the resulting tetherin upregulation did not inhibit cell-cell spread of either WT or ΔVpu virus (Fig. 4A and D). When assayed by both real-time PCR and flow cytometry, Jurkat-pNL4.3 WT cells treated with IFN showed a slight, 2-fold increase in HIV-1 transmission, but this did not reach statistical significance. Sim-

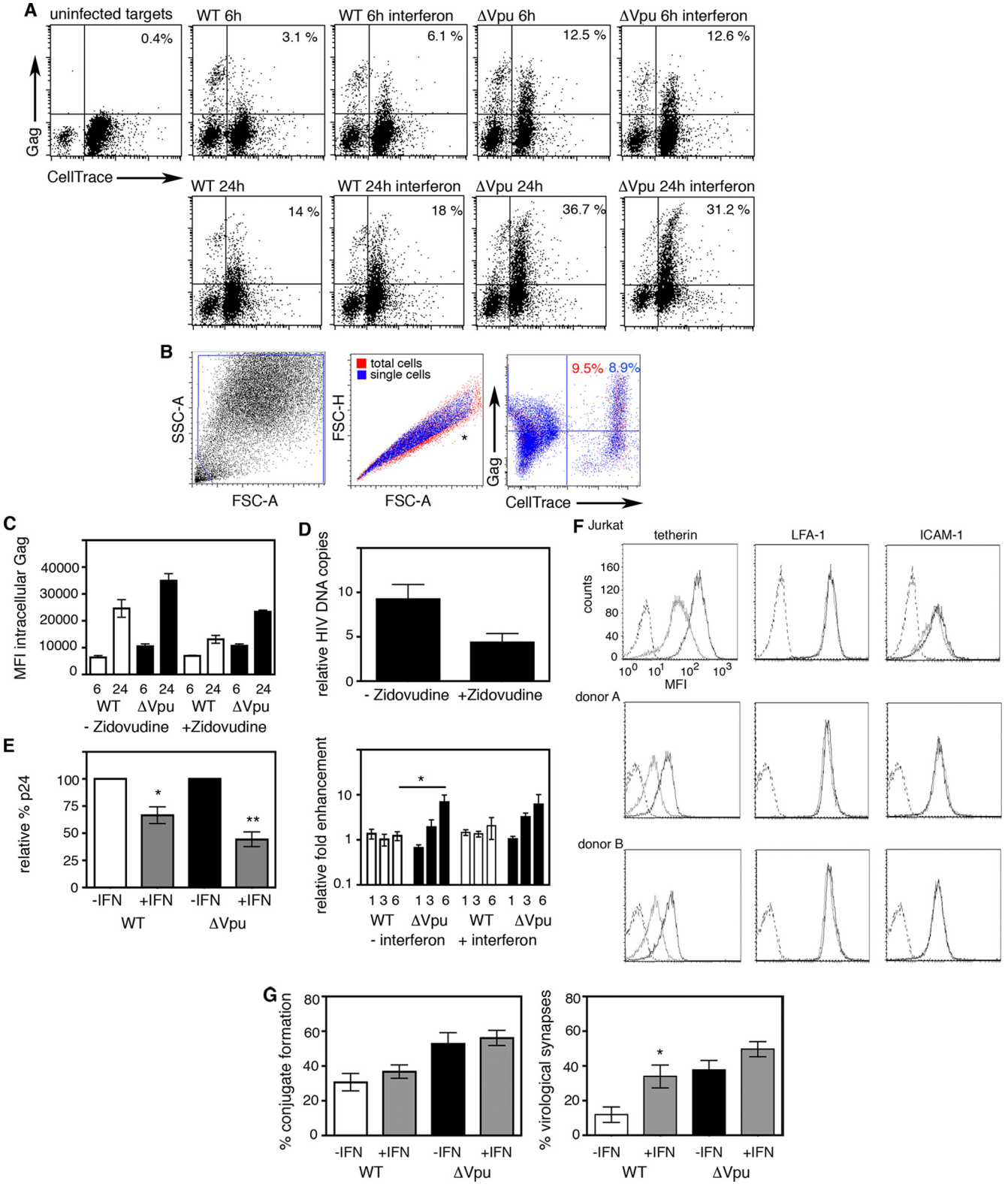

ilarly, IFN treatment did not inhibit cell-cell interactions or VS formation but rather increased the frequency of VS formation by Jurkat-pNL4.3 WT cells 2.3-fold ($P < 0.05$) (Fig. 4G), correlating with the observed slight increase in cell-cell spread. VS formation by ΔVpu virus was similarly uninhibited by IFN treatment compared to cells that were not exposed to IFN, indicating that tetherin does not inhibit VS formation and that upregulating tetherin expression on the cells that already ex-

press tetherin to relatively high levels does not affect cell-cell spread in this assay system. We also confirmed that while IFN treatment increased the surface expression of tetherin on Jurkat T cells and primary T cells, there was no effect on surface expression of the adhesion molecules LFA-1 and ICAM-1, which also contribute to cell-cell spread at the VS (Fig. 4F) (28). Taken together, these data indicate that upregulating endogenous tetherin on T cells does not prevent productive T cell-T cell spread of HIV-1.

siRNA knockdown of tetherin reduces cell-cell spread of ΔVpu virus. If cell-cell spread of HIV-1 is restricted by tetherin, it would be expected that siRNA knockdown of endogenous tetherin might increase transmission of Vpu-defective HIV-1. Conversely, if tetherin does not inhibit HIV-1 dissemination at the VS, then siRNA knockdown might be expected to have little effect on transmission. To differentiate between these two possibilities, Jurkat T cells were nucleofected with siRNA targeting tetherin and infected with pNL4.3ΔVpu or WT virus, and cell-cell spread was measured at 72 h postinfection by real-time PCR. Flow cytometry confirmed that anti-tetherin siRNA reduced plasma membrane expression by an average of 50 to 70% (Fig. 5A). Moreover, cells treated with either anti-tetherin or control siRNA were susceptible to infection by HIV-1 (data not shown). Analysis of direct cell-cell spread of HIV-1 by real-time PCR showed that siRNA knockdown of tetherin did not increase cell-cell transmission of pNL4.3ΔVpu or WT virus compared to cells treated with control siRNA (Fig. 5B). In contrast, we observed that tetherin knockdown decreased cell-cell spread of both WT and pNL4.3ΔVpu virus by up to 55%. To investigate this further, Jurkat T cells were treated with control or tetherin siRNA and infected with WT or ΔVpu virus, and conjugate and VS formation was quantified (Fig. 5C). Knockdown of tetherin in effector T cells had a little effect on conjugate formation but significantly reduced VS formation by ΔVpu-infected cells, by approximately 45% compared to cells treated with control siRNA ($P < 0.01$). Similarly, a 50% reduction in WT VS formation was also observed, but this did not reach statistical significance ($P > 0.05$). It should be noted that VSs could sometimes be observed without detectable tetherin enrichment at sites of cell-cell contact following RNAi (Fig. 5D), with the caveat that tetherin localization at the VS following knockdown may be below the level of detection by immunofluorescence microscopy. Thus, rather than inhibiting transmission, tetherin may partially contribute to the HIV-1 VS.

Because tetherin knockdown with RNAi appeared to reduce cell-cell spread of WT HIV-1 that antagonizes tetherin, we wished to examine to what extent antagonized tetherin was downregulated from the surface of T cells infected with HIV-1 in the absence of RNAi. Infected T cells were stained for surface tetherin and intracellular Gag, and the relative proportions of tetherin-expressing infected and un-

FIG. 4. Quantification of cell-cell spread. (A) Flow cytometric analysis of Gag transfer. Jurkat T cells infected with pNL4.3 WT or ΔVpu were either left untreated or pretreated with 500 U/ml interferon for 24 h and mixed with dye-labeled target T cells, and the percentage of Gag^+ target cells was measured by flow cytometry. Data are from two independent experiments performed in duplicate, and values show the mean percentages of Gag^+ dye-labeled target cells with the SEMs. Infected cells were used when >80% of the donor cells were routinely Gag^+ by flow cytometry. (B) Comparison of total-cell and single-cell gating. Jurkat T cells infected with pNL4.3 WT or ΔVpu were mixed with CellTrace dye-labeled target T cells, data were acquired using an LSRII flow cytometer with FACSDiva software, and the percentage of Gag^+ dye-labeled target cells was quantified using FlowJo. The first gate was applied to define the total, live cell population (far left panel), and this population was then analyzed using FSC-A versus FSC-H for doublet discrimination and a second gate applied to differentiate single cells (blue) from the total population (red) to exclude doublets from analysis (middle panel). Note that there are few cells in the position expected for the doublet population (denoted with an asterisk). The overlay (right panel) shows a comparison of cell-cell transfer to target cells when gating on the total cell population (red) or with single cells only (blue). Values denote the percentages of Gag^+ target cells identified when gating on total cells or single cells. A representative example of cell-cell spread of ΔVpu virus after 6 h of coculture with target cells is shown; similar results were obtained with WT virus. (C) Zidovudine partially reduces intracellular Gag staining in newly infected targets following cell-cell spread. Dye-labeled target cells were either left untreated or pretreated with the reverse transcriptase inhibitor zidovudine for an hour at 37°C prior to being mixed with WT-infected (white) or ΔVpu-infected (black) cells for 6 h or 24 h and subsequent intracellular Gag staining. Data show the mean fluorescence intensity of intracellular Gag staining in the newly infected Gag^+ dye-labeled target cell population in the presence and absence of zidovudine following cell-cell transmission. Data were acquired using an LSRII flow cytometer as described above to exclude doublets and are means from two independent experiments with the SEMs. (D) Quantitative real-time PCR of cell-cell spread. The lower panel shows results from Jurkat T cells infected with pNL4.3 (white bars) or ΔVpu (black bars) and either left untreated or pretreated with 500 U/ml interferon for 24 h, mixed with uninfected target T cells, and incubated for 1, 3, and 6 h prior to lysis and extraction of DNA. Real-time PCR was performed using *pol* primers to quantify *de novo* HIV-1 DNA synthesis as a measure of HIV-1 cell-cell spread. Data were normalized to human serum albumin (HSA). The values obtained at $t = 0$ h (baseline) were subtracted from the test values, and data are shown as the relative fold enhancement over 0 h. Data are from four independent experiments, and error bars show the SEMs. Experiments were performed when >90% of the donor cells were Gag^+ by flow cytometry. The upper panel shows data from experiments in which target cells were pretreated with the reverse transcriptase inhibitor zidovudine for an hour at 37°C prior to incubation with ΔVpu-infected T cells for 6 h. The values obtained at $t = 0$ h (baseline) were subtracted from the test values, and data are shown as the relative HIV DNA copy number normalized to human serum albumin (HSA). Error bars are the SEMs from two independent experiments. (E) Confirmation that interferon treatment reduces cell-free virus release. Jurkat-pNL4.3 WT (white bar) and Jurkat-ΔVpu (black bar) cells were either untreated or incubated with 500 U/ml interferon (gray bars) for 24 h, and cell-free supernatants were assayed for viral content by p24 ELISA. Data are relative percent p24 levels with untreated cells normalized to 100% and are means from four independent experiments with the SEMs. (F) IFN-β treatment upregulates surface tetherin but not adhesion molecule expression on T cells. Jurkat cells and primary $CD4^+$ T cells from two different donors (A and B) were either left untreated (gray lines) or incubated for 24 h with 500 U/ml of IFN-β in the growth medium (black lines) and surface stained for tetherin (left panels), LFA-1 (middle panels), and ICAM-1 (right panels). Unstained cells are also depicted (broken lines). Representative histograms are shown. (G) VS formation is not inhibited by interferon treatment. Jurkat-pNL4.3 WT and Jurkat-ΔVpu cells were either treated with interferon or left untreated and quantified for conjugate (left panel) and VS (right panel) formation as described for Fig. 2. Data are from three independent experiments, and error bars show SEMs. Jurkat-pNL4.3 WT: untreated, white bars ($n = 179$); with interferon, gray bars ($n = 261$). Jurkat-ΔVpu: untreated, black bars ($n = 162$); with interferon, gray bars ($n = 221$). *, $P < 0.05$; **, $P < 0.01$; ***, $P < 0.005$; ****, $P < 0.001$.

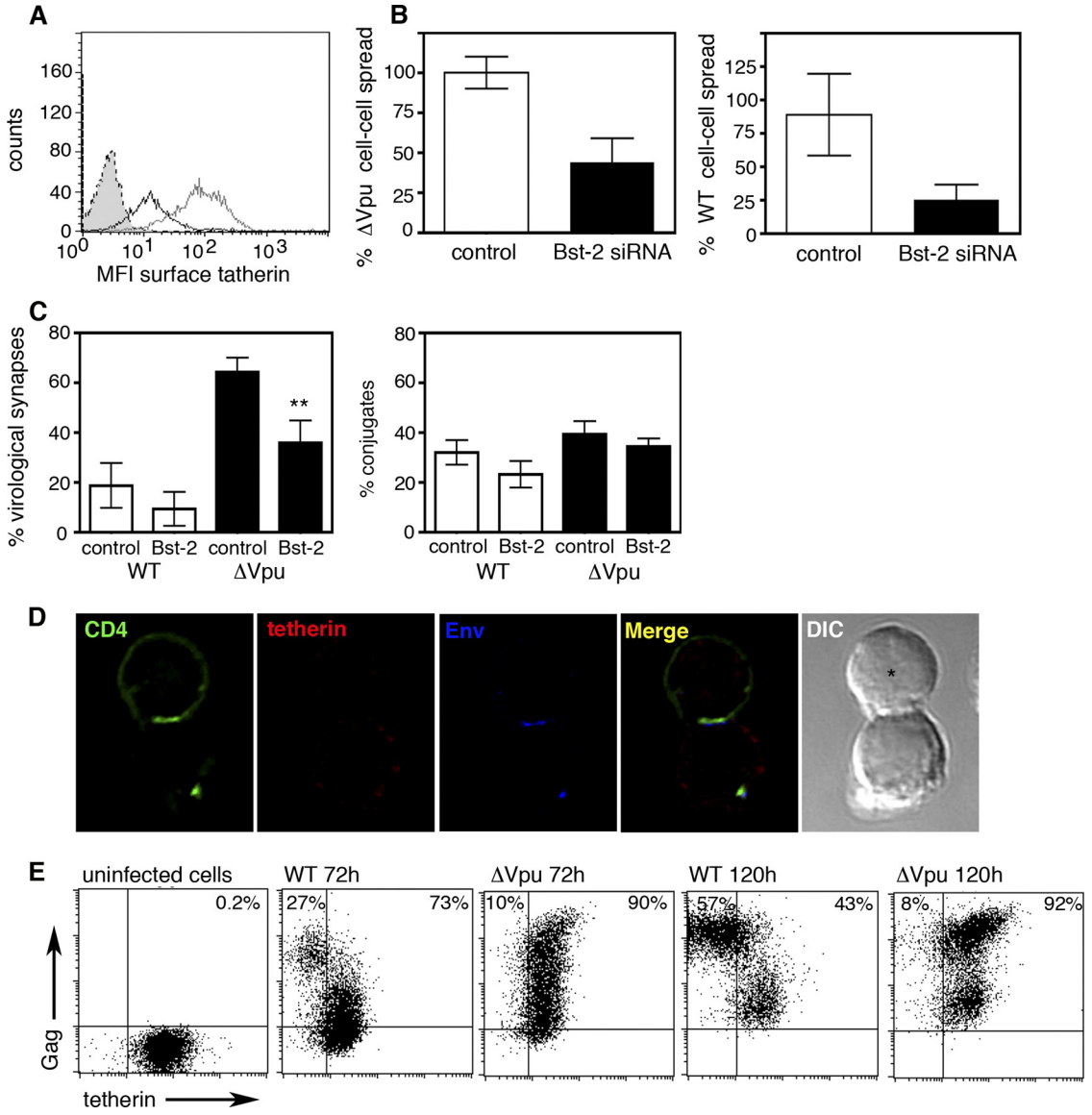

FIG. 5. siRNA knockdown of tetherin/Bst-2 reduces cell-cell spread. (A) Flow cytometry of tetherin knockdown. Jurkat T cells were nucleofected with control siRNA (gray line) or siRNA targeting tetherin (black line), and 48 h later surface tetherin expression was measured by flow cytometry. The gray-filled histogram shows nucleofected cells stained with the secondary antibody only. Data from a representative experiment are shown. (B) siRNA knockdown of tetherin reduces cell-cell spread of HIV-1. Jurkat T cells were nucleofected with siRNA targeting tetherin/Bst-2 (black bars) or control siRNA (white bars), and 24 h later cells were infected with ΔVpu (left panel) or WT (right panel) virus and cell-cell spread measured by real-time PCR as described above. Data are from three independent experiments and show mean relative percent cell-cell spread with the SEM. (C) Quantification of VS formation after siRNA knockdown. Jurkat-pNL4.3 WT cells and Jurkat-ΔVpu cells were nucleofected with siRNA and infected with virus as described above, and after 72 h cells were mixed with target T cells and quantified for VS (left panel) and conjugate (right panel) formation as described for Fig. 2. Data are means from three independent experiments with the SEMs. Jurkat-pNL4.3 WT control siRNA, $n = 129$; Jurkat-pNL4.3 WT BST-2 siRNA, $n = 108$; Jurkat-ΔVpu control siRNA, $n = 161$; Jurkat-ΔVpu BST-2 siRNA, $n = 251$. *, $P < 0.05$; **, $P < 0.01$; ***, $P < 0.005$; ****, $P < 0.001$. (D) Visualization of the VS after tetherin siRNA treatment. Jurkat T cells were treated with anti-tetherin siRNA and infected with ΔVpu virus, and VS formation was examined by IF and LSCM. CD4 is green, surface tetherin is red, and Env is blue. Target cells are indicated with an asterisk. (E) Flow cytometry of surface tetherin expression on infected Jurkat T cells. Jurkat T cells were infected with pNL4.3 WT or ΔVpu, surface stained for tetherin and intracellular Gag, and analyzed by flow cytometry. Data from a representative experiment are shown.

infected cells were quantified by flow cytometry (Fig. 5E). As expected, surface expression of tetherin was unchanged on ΔVpu-infected cells compared to uninfected control cells (90% tetherin positive [MFI = 24] compared to 86% tetherin positive [MFI = 22]) at 72 h postinfection, the time point at which infected cells were used to assay cell-cell spread following RNAi. In contrast, while the majority of WT Gag^+ cells still expressed tetherin at 72 h (73%; MFI = 21) a minor but distinct Gag^+ $tetherin^-$ population was apparent (27%; MFI = 4.6), which expanded to 57% by 120 h postinfection (MFI = 4.4). The fact that most of our WT-infected cells still expressed some tetherin at the

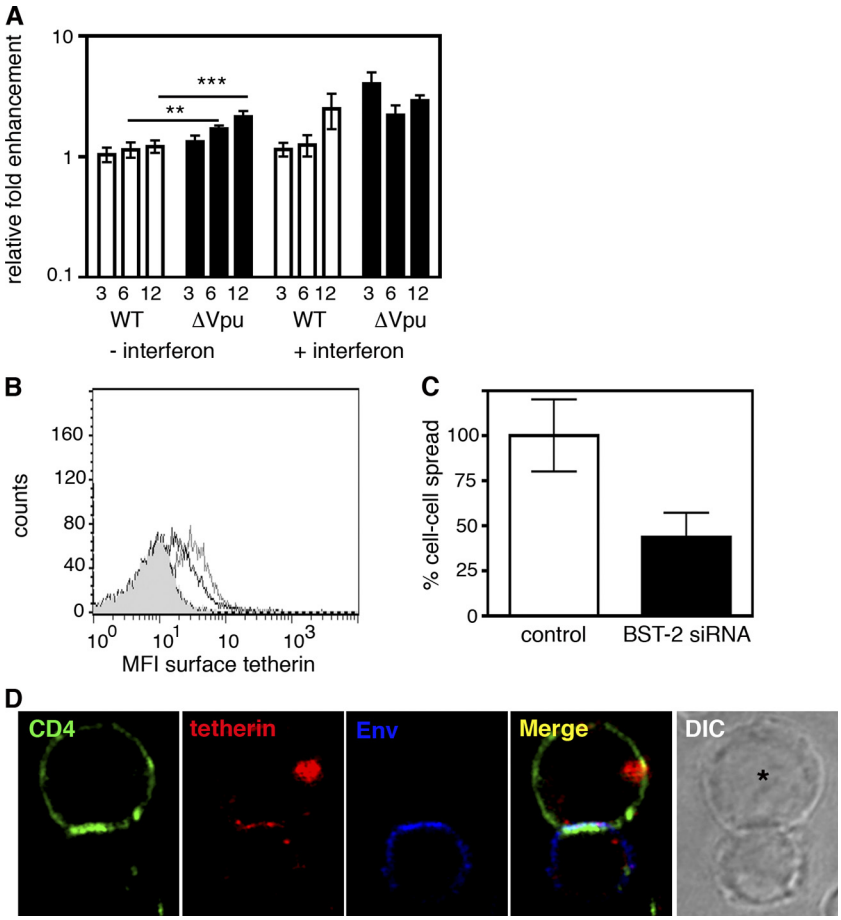

FIG. 6. Cell-cell spread of HIV-1 from infected primary $CD4^+$ T cells. (A) Primary $CD4^+$ T cells infected with pNL4.3 WT (white bars) or ΔVpu (black bars) were either left untreated or pretreated with 500 U/ml interferon for 24 h before being mixed with uninfected target T cells and incubated for 3, 6, and 12 h prior to real-time PCR analysis of cell-cell spread as described for Fig. 4. Data are from at least three independent experiments performed with three different donors, and error bars show the SEMs. *, $P < 0.05$; **, $P < 0.01$; ***, $P < 0.005$; ****, $P < 0.001$. (B) Flow cytometry of tetherin knockdown. Primary $CD4^+$ T cells were nucleofected with control siRNA (gray line) or siRNA targeting tetherin (black line), and 48 h later surface tetherin expression was measured by flow cytometry. The gray-filled histogram shows nucleofected cells stained with the secondary antibody only. Data from a representative experiment are shown. (C) siRNA knockdown of tetherin reduces cell-cell spread from infected primary $CD4^+$ T cells. Primary T cells were nucleofected with siRNA targeting tetherin/Bst-2 (black bars) or control siRNA (white bars), and 24 h later cells were infected with ΔVpu HIV-1 and cell-cell spread measured by real-time PCR as described above. Data are from two independent donors and show the mean relative percentage cell-cell spread with the SEM. (D) Tetherin is enriched on primary $CD4^+$ T cells at the VS. Primary T cells infected with ΔVpu virus were mixed with uninfected target T cells and incubated for an hour at 37°C in the presence of MAbs against Env (blue), CD4 (green), and tetherin (red). Results from a representative image from experiments performed with two different donors are shown.

plasma membrane at 72 h postinfection may explain in part why we could detect an effect of RNAi knockdown of tetherin on cell-cell spread of WT virus.

Cell-cell spread of HIV-1 from primary $CD4^+$ T cells. Although the Jurkat T cell line is a useful model for studying HIV-1 infection *in vitro*, primary $CD4^+$ T cells are the natural targets for HIV-1 *in vivo*. To address whether primary T cells are similarly affected by Vpu and tetherin expression, $CD4^+$ T cells were isolated from healthy donors and infected with either pNL4.3 WT or pNL4.3ΔVpu, and cell-cell spread was quantified by real-time PCR (Fig. 6A). In order to directly compare cells infected with Vpu-expressing and nonexpressing HIV-1 from multiple donors, we used an immortalized T cell line as uninfected targets to remove any contribution from polymorphisms that may affect HIV-1 entry and reverse transcription, since this has been shown to be a suitable substitute in this assay (41). In agreement with our previous results, ΔVpu virus could be transmitted by cell-cell spread in the presence of tetherin, and this was not inhibited by IFN treatment and tetherin upregulation. Again, there was a modest but significant increase in cell-cell spread by ΔVpu virus compared to WT virus at both 6 h (1.7- compared to 1-fold increase over baseline; $P = 0.01$) and 12 h (2.1- compared to 1.2-fold increase over baseline; $P = 0.005$), and cell-cell spread of WT was also somewhat more efficient following IFN treatment ($P = 0.04$), but this was not seen with ΔVpu virus ($P = 0.2$). Moreover, siRNA knockdown of endogenous tetherin in primary $CD4^+$ T cells reduced surface expression by approximately 30% (Fig. 6B) but did not increase cell-cell spread, and in good correlation with results obtained with Jurkat T cells,

siRNA knockdown of tetherin reduced cell-cell spread by 56% (Fig. 6C). Finally, tetherin could also be detected at the VS on HIV-1-infected primary $CD4^+$ T cells colocalizing with Env at sites of cell-cell contact (Fig. 6D).

DISCUSSION

Cellular restriction factors target HIV-1 at different stages of the viral life cycle to inhibit or limit virus replication, often in response to IFN induction (46). HIV-1 has evolved a number of mechanisms to counteract restriction factors, including expression of the accessory proteins Vif (which inhibits APOBEC3-mediated cytidine deamination of viral transcripts) (69) and Vpu (which overcomes tetherin-mediated inhibition of HIV-1 release) (49, 81). During HIV-1 cell-cell spread, viral assembly and egress are polarized toward the target cell (7, 22, 27, 55), and so we hypothesized that cell-cell spread of HIV-1 between T cells may be able to overcome restriction by temporally and spatially saturating inhibitory proteins. Conversely, evidence suggests that cell-cell spread of HIV-1 occurs by budding of virions from the plasma membrane of infected cells into the synaptic cleft (22, 27); thus, aspects of particle release and attachment and entry into target cells are mechanistically analogous to cell-free infection. For this reason it is also possible that restriction factors may be equally active against direct cell-cell transfer. With this in mind, we investigated whether cell-cell spread of HIV-1 can overcome restriction by the most recently described restriction factor, tetherin, and by extension whether Vpu is necessary for transmission at the VS. Our data using Vpu-defective virus, interferon-induced tetherin upregulation, and RNAi suggest that unantagonized tetherin is present at the T cell VS but that it does not significantly inhibit cell-cell interactions or VS formation. Despite efficient VS formation by Vpu-defective HIV-1, because tetherin physically links virions to the plasma membrane (49, 56), it remained possible that infection of target cells could be inhibited due to restriction of infectious particle release at sites of cell-cell contact even in the presence of efficient VS formation. Our data suggest that this is not case for the following reasons: first, we could detect transfer of HIV-1 Gag to target cells by flow cytometry, the production of newly synthesized reverse transcripts by quantitative real-time PCR, and the synthesis of new viral Gag protein when T cells infected with ΔVpu virus were mixed with uninfected T cells, thus demonstrating that HIV-1 can be productively transmitted to target cells across the VS in the presence of endogenous tetherin; second, IFN treatment of infected T cells did not inhibit Gag transfer or the synthesis of HIV-1 reverse transcripts, indicating that HIV-1 can be efficiently transmitted even after tetherin upregulation by IFN; third, siRNA knockdown of tetherin did not increase transmission of HIV-1 at the T cell VS; and fourth, tethered viruses are fully infectious and thus tetherin does not appear to inhibit virus-cell fusion as a consequence of virion incorporation. Taking our findings together, we conclude that HIV-1 can disseminate by direct T cell-T cell transfer in the presence of endogenous tetherin expressed on the virus-producing T cell. In the same cellular system, tetherin restricts the release of cell-free virus particles. It has previously been reported that cell-cell spread of HIV-1 is less sensitive than cell-free infection to TRIM5α restriction (58), and so in addition to promoting more rapid infection kinetics, another advantage of cell-cell spread may be to allow HIV-1 to disseminate in the presence of host restriction factors.

Tetherin is polarized on epithelial cells, where it modulates actin dynamics and provides a link between the actin network and lipid rafts (60). Tetherin binding to the BAR-RacGAP protein RICH2 appears to be essential for subapical F-actin organization, and perturbation of this interaction increases Rac activation and causes loss of apical microvilli (60). Tetherin is also reported to be present in lipid rafts (34), which are sites of HIV-1 assembly at the plasma membrane (4, 50, 51), and maintenance of the integrity of lipid rafts and the actin cytoskeleton are required for efficient HIV-1 dissemination at the VS (29, 30, 55). Rather than increasing HIV-1 dissemination, we found that depleting surface tetherin by nucleofecting T cells with siRNA reduced VS formation and cell-cell spread of HIV-1, in keeping with the idea that tetherin may play a more general role in T cells via interacting with the actin cytoskeleton and plasma membrane microdomains. If tetherin does indeed modulate cytoskeletal dynamics and plasma membrane organization, this raises the question of how WT strains of HIV-1 spread by cell-cell transmission in the face of Vpu expression (6, 22, 27, 64, 74). Mutants of Vpu that lack the phosphoserine acceptors that mediate binding to βTrCP1/2 maintain tetherin antagonism in T cells but fail to remove it from the plasma membrane and degrade it (13), suggesting that Vpu may antagonize tetherin by excluding it from sites of virus assembly. Indeed, it has been proposed that tetherin degradation may not be necessary for Vpu antagonism of its effects on virus release, and in some systems degradation appears to be quite inefficient (10). We found that siRNA knockdown of tetherin impaired WT HIV-1 dissemination by cell-cell spread, indicating that loss of tetherin from the plasma membrane may negatively affect T cell function, at least in the context of HIV-1 transmission. We also detected a decrease in surface tetherin expression on cells infected with WT virus but not Vpu-defective HIV-1, and thus we cannot exclude the possibility of temporal, as well as spatial, effects of tetherin antagonism in our system. Future work to elucidate the normal cellular function of tetherin/BST2 and antagonism by Vpu will undoubtedly shed light on the role of tetherin in cell-cell interactions and HIV-1 dissemination.

Interestingly, we observed that Vpu-defective HIV-1 appears to disseminate more efficiently by direct cell-cell transfer, and we hypothesize that this is likely due, at least in part, to increased VS and polysynapse formation. In support of our observations, Gummurulu et al. have previously reported that more rapid cell-cell spread of HIV-1 occurs in culture following mutation in *vpu* (19), while data from important early studies characterizing the phenotype of Vpu-defective HIV-1 also noted that Vpu-defective virus was able to spread in culture (33, 68, 77, 80, 85), hinting that Vpu may contribute to replication *in vitro* by mechanisms involving cell-cell transfer. We hypothesize that by preventing the release of virions from the cell surface, unantagonized tetherin could trigger more Env-dependent VS to evolve. In this model, mature infectious virions remaining associated with the producer cell could then be poised to engage and recruit CD4 and coreceptor on the target cell, contributing to more rapid virus transmission. The presence of preformed infectious virus accumulating at the cell

surface could also increase replication kinetics by obviating any lag in recruiting viral proteins to sites of *de novo* virus assembly at the VS (22). In support of this, Pais-Correia et al. have described the presence of extracellular viral assemblies (or biofilms) on the surface of HTLV-1-infected lymphocytes that mediate cell-cell spread (53). Notably, these biofilms contain tetherin, among other cellular proteins. HTLV-1 disseminates exclusively by cell-cell spread at virological synapses (24) and appears to be resistant to tetherin-mediated restriction, but it does not encode a known tetherin antagonist, and it is tempting to speculate that HTLV-1 may have adapted to exploit tetherin to enhance viral dissemination under certain conditions. Furthermore, directional spread of the related retrovirus murine leukemia virus (MLV) between fibroblasts is mediated in part by the transmission of surface-associated virions that are nonspecifically attached to the surface of the virus-producing cell via interactions with glycosaminoglycans (70). MLV, like HTLV-1, is not known to encode a tetherin antagonist (14); however, the effect of tetherin on directional cell-cell spread of MLV is not clear at present. While we have hypothesized that tethered particles may contribute, at least in part, to transmission of Vpu-defective HIV-1, we cannot exclude the possibility that increased Env expression on ΔVpu-infected cells may be masking some restriction of virus spread; however, we did not observe any increase in HIV-1 cell-cell transmission when endogenous tetherin was depleted using siRNA, nor was spread restricted following tetherin upregulation with interferon, suggesting that tetherin does not prevent functional T cell-T cell transfer.

While this paper was in preparation Casartelli et al. also reported that tetherin accumulates at sites of cell-cell contact and does not prevent virological synapse formation (5). In contrast to our results, it was reported that productive cell-cell spread was sensitive to tetherin-mediated restriction and that virions produced from cells expressing tetherin were transmitted by cell-cell spread as large aggregates that had reduced infectivity (5). While aspects of these two studies are in broad agreement, there are conflicting data; most notably, we found that cell-cell spread of HIV-1 between T cells is not restricted and that T cells can be productively infected with Vpu-defective virus following cell-cell spread. Moreover, we did not detect any loss of viral infectivity *per se* when virions were produced from T cells expressing endogenous tetherin. We believe that one possible explanation for the differences between that study and ours could be cell type-dependent variation in the levels of tetherin expression, since the experimental approaches are broadly similar. Here we have used Jurkat T cells and primary T cells expressing endogenous tetherin. T cells express comparatively less tetherin than HeLa cells or 293T cells transfected with a recombinant plasmid (45, 48, 49, 81), and it is possible that under conditions of high tetherin expression HIV-1 cell-cell spread may be impaired, whereas at lower levels tetherin may not restrict, or may even contribute to, cell-cell spread. Contrasting results were also obtained in the two studies when T cells were used, and this too could be attributed to variation in tetherin expression between the different T cell lines and clones, a phenotype that Miyagi et al. have previously reported (45). Moreover, we cannot exclude differences in the infection kinetics in donor cell populations and in the molecular mechanisms of cell-cell spread between different donor and target cell combinations (e.g., T cell-T cell versus epithelial cell-T cell) as contributing factors.

Since tetherin antagonism is a highly conserved attribute of primate immunodeficiency viruses, be it associated with the Vpu, Nef, or Env genes (20, 26, 36, 46, 86), our data raise the possibility that for optimal host-to-host transmission and systemic spread, HIV-1 requires a balance between cell-cell spread and the production of cell-free virions. The Vpu open reading frame reading frame is maintained in transmitted founder viruses (63), and recent evidence suggests that of the three known zoonotic transfers of the simian immunodeficiency virus SIVcpz (whose Nef proteins antagonize chimpanzee but not human tetherin), only those that became HIV-1 group M acquired the ability to target human tetherin in their Vpu proteins (66). HIV-1 group M, unlike groups N and O, was able to become a human pandemic virus rather than a localized epidemic virus, suggesting that attributes such as Vpu function may have favored human-to-human transmission. Once infection is established in lymphoid tissues such as the gut-associated lymphoid tissue (GALT) (a major site of HIV-1 replication) (3, 18, 43, 57, 67, 83), cell-cell transfer may be an important mode of HIV-1 dissemination, and one might speculate that the Vpu antagonism of tetherin may be less important at this stage. Alternatively, tetherin may restrict cell-cell spread in other cellular systems such as macrophages and dendritic cells, and cell type-specific effects of interferon treatment on retroviral infection have been reported (15). The interferon-inducible nature of restriction factors such as tetherin and TRIM5α (46) has raised the possibility of using interferon-based therapy to upregulate the natural antiviral activity of cells; however, cell-cell spread of HIV-1 is less sensitive than cell-free infection to TRIM5α restriction (58), and our data additionally suggest that cell-cell spread is not efficiently restricted by tetherin. It is also interesting to note that interferon is ineffective at limiting viral spread in *in vitro* culture due to cell-cell spread (84). If cell-cell spread of HIV-1 can overcome restriction factors *in vivo*, even in part, then this might contribute to the failure of IFN treatment in reducing the viral load in HIV-1-positive patients (11, 21, 23, 32, 35, 52, 59, 72, 76), suggesting that such an antiviral strategy may be more complicated than anticipated.

ACKNOWLEDGMENTS

We thank Mike Shaw (University of Oxford) for assistance with electron microscopy. The following reagents were obtained through the AIDS Research and Reference Reagent Program, Division of AIDS, NIAID, NIH: HIV-1_{NL4-3} Vpu antiserum from Frank Maldarelli and Klaus Strebel and zidovudine from the Division of AIDS. We also acknowledge reagents obtained from the Centralized Facility for AIDS Reagents supported by EU Programme EVA (contract QLKZ-CT-1999-00609) and the United Kingdom Medical Research Council.

C.J. conceived the project, performed experiments, analyzed data, and wrote the paper. N.J.B. performed experiments and analyzed data. S.J.D.N. analyzed data and wrote the paper.

This work was funded by a Medical Research Council CDA to C.J. (G0800312) and a Wellcome Trust RCDF to S.J.D.N. (WT082774MA).

REFERENCES

1. **Blasius, A. L., E. Giurisato, M. Cella, R. D. Schreiber, A. S. Shaw, and M. Colonna.** 2006. Bone marrow stromal cell antigen 2 is a specific marker of type I IFN-producing cells in the naive mouse, but a promiscuous cell surface antigen following IFN stimulation. J. Immunol. **177:**3260–3265.

2. **Bosch, B., B. Grigorov, J. Senserrich, B. Clotet, J. L. Darlix, D. Muriaux, and J. A. Este.** 2008. A clathrin-dynamin-dependent endocytic pathway for the uptake of HIV-1 by direct T cell-T cell transmission. Antiviral Res. **80:**185–193.
3. **Brenchley, J. M., T. W. Schacker, L. E. Ruff, D. A. Price, J. H. Taylor, G. J. Beilman, P. L. Nguyen, A. Khoruts, M. Larson, A. T. Haase, and D. C. Douek.** 2004. CD4+ T cell depletion during all stages of HIV disease occurs predominantly in the gastrointestinal tract. J. Exp. Med. **200:**749–759.
4. **Campbell, S. M., S. M. Crowe, and J. Mak.** 2001. Lipid rafts and HIV-1: from viral entry to assembly of progeny virions. J. Clin. Virol. **22:**217–227.
5. **Casartelli, N., M. Sourisseau, J. Feldmann, F. Guivel-Benhassine, A. Mallet, A.-G. Marcelin, J. Guatelli, and O. Schwartz.** 2010. Tetherin restricts productive HIV-1 cell-to-cell transmission. PLoS Pathog. **6:**e1000955.
6. **Chen, P., W. Hubner, M. A. Spinelli, and B. K. Chen.** 2007. Predominant mode of human immunodeficiency virus transfer between T cells is mediated by sustained Env-dependent neutralization-resistant virological synapses. J. Virol. **81:**12582–12595.
7. **Deschambeault, J., J. P. Lalonde, G. Cervantes-Acosta, R. Lodge, E. A. Cohen, and G. Lemay.** 1999. Polarized human immunodeficiency virus budding in lymphocytes involves a tyrosine-based signal and favors cell-to-cell viral transmission. J. Virol. **73:**5010–5017.
8. **Dimitrov, D. S., R. L. Willey, H. Sato, L. J. Chang, R. Blumenthal, and M. A. Martin.** 1993. Quantitation of human immunodeficiency virus type 1 infection kinetics. J. Virol. **67:**2182–2190.
9. **Douglas, J. L., K. Viswanathan, M. N. McCarroll, J. K. Gustin, K. Fruh, and A. V. Moses.** 2009. Vpu directs the degradation of the human immunodeficiency virus restriction factor BST-2/Tetherin via a (beta)TrCP-dependent mechanism. J. Virol. **83:**7931–7947.
10. **Dube, M., B. B. Roy, P. Guiot-Guillain, J. Binette, J. Mercier, A. Chiasson, and E. A. Cohen.** 2010. Antagonism of tetherin restriction of HIV-1 release by Vpu involves binding and sequestration of the restriction factor in a perinuclear compartment. PLoS Pathog. **6:**e1000856.
11. **Frissen, P. H., F. de Wolf, P. Reiss, P. J. Bakker, C. H. Veenhof, S. A. Danner, J. Goudsmit, and J. M. Lange.** 1997. High-dose interferon-alpha2a exerts potent activity against human immunodeficiency virus type 1 not associated with antitumor activity in subjects with Kaposi's sarcoma. J. Infect. Dis. **176:**811–814.
12. **Goffinet, C., I. Allespach, S. Homann, H. M. Tervo, A. Habermann, D. Rupp, L. Oberbremer, C. Kern, N. Tibroni, S. Welsch, J. Krijnse-Locker, G. Banting, H. G. Krausslich, O. T. Fackler, and O. T. Keppler.** 2009. HIV-1 antagonism of CD317 is species specific and involves Vpu-mediated proteasomal degradation of the restriction factor. Cell Host Microbe **5:**285–297.
13. **Goffinet, C., S. Homann, I. Ambiel, N. Tibroni, D. Rupp, O. T. Keppler, and O. T. Fackler.** 2010. Antagonism of CD317 restriction of human immunodeficiency virus type 1 (HIV-1) particle release and depletion of CD317 are separable activities of HIV-1 Vpu. J. Virol. **84:**4089–4094.
14. **Goffinet, C., S. Schmidt, C. Kern, L. Oberbremer, and O. T. Keppler.** 2010. Endogenous CD317/tetherin limits replication of HIV-1 and murine leukemia virus in rodent cells and is resistant to antagonists from primate viruses. J. Virol. **84:**11374–11384.
15. **Goujon, C., and M. H. Malim.** 2010. Characterization of the alpha interferon-induced postentry block to HIV-1 infection in primary human macrophages and T cells. J. Virol. **84:**9254–9266.
16. **Gousset, K., S. D. Ablan, L. V. Coren, A. Ono, F. Soheilian, K. Nagashima, D. E. Ott, and E. O. Freed.** 2008. Real-time visualization of HIV-1 GAG trafficking in infected macrophages. PLoS Pathog. **4:**e1000015.
17. **Groot, F., S. Welsch, and Q. J. Sattentau.** 2008. Efficient HIV-1 transmission from macrophages to T cells across transient virological synapses. Blood **111:**4660–4663.
18. **Guadalupe, M., E. Reay, S. Sankaran, T. Prindiville, J. Flamm, A. McNeil, and S. Dandekar.** 2003. Severe CD4+ T-cell depletion in gut lymphoid tissue during primary human immunodeficiency virus type 1 infection and substantial delay in restoration following highly active antiretroviral therapy. J. Virol. **77:**11708–11717.
19. **Gummuluru, S., C. M. Kinsey, and M. Emerman.** 2000. An in vitro rapid-turnover assay for human immunodeficiency virus type 1 replication selects for cell-to-cell spread of virus. J. Virol. **74:**10882–10891.
20. **Gupta, R. K., P. Mlcochova, A. Pelchen-Matthews, S. J. Petit, G. Mattiuzzo, D. Pillay, Y. Takeuchi, M. Marsh, and G. J. Towers.** 2009. Simian immunodeficiency virus envelope glycoprotein counteracts tetherin/BST-2/CD317 by intracellular sequestration. Proc. Natl. Acad. Sci. U. S. A. **106:**20889–20894.
21. **Hatzakis, A., P. Gargalianos, V. Kiosses, M. Lazanas, V. Sypsa, C. Anastassopoulou, V. Vigklis, H. Sambatakou, C. Botsi, D. Paraskevis, and C. Stalgis.** 2001. Low-dose IFN-alpha monotherapy in treatment-naive individuals with HIV-1 infection: evidence of potent suppression of viral replication. J. Interferon Cytokine Res. **21:**861–869.
22. **Hubner, W., G. P. McNerney, P. Chen, B. M. Dale, R. E. Gordon, F. Y. Chuang, X. D. Li, D. M. Asmuth, T. Huser, and B. K. Chen.** 2009. Quantitative 3D video microscopy of HIV transfer across T cell virological synapses. Science **323:**1743–1747.
23. **Hulton, M. R., D. L. Levin, and L. S. Freedman.** 1992. Randomized, placebo-controlled, double-blind study of low-dose oral interferon-alpha in HIV-1 antibody positive patients. J. Acquir. Immune Defic. Syndr. **5:**1084–1090.
24. **Igakura, T., J. C. Stinchcombe, P. K. Goon, G. P. Taylor, J. N. Weber, G. M. Griffiths, Y. Tanaka, M. Osame, and C. R. Bangham.** 2003. Spread of HTLV-I between lymphocytes by virus-induced polarization of the cytoskeleton. Science **299:**1713–1716.
25. **Iwabu, Y., H. Fujita, M. Kinomoto, K. Kaneko, Y. Ishizaka, Y. Tanaka, T. Sata, and K. Tokunaga.** 2009. HIV-1 accessory protein Vpu internalizes cell-surface BST-2/tetherin through transmembrane interactions leading to lysosomes. J. Biol. Chem. **284:**35060–35072.
26. **Jia, B., R. Serra-Moreno, W. Neidermyer, A. Rahmberg, J. Mackey, I. B. Fofana, W. E. Johnson, S. Westmoreland, and D. T. Evans.** 2009. Species-specific activity of SIV Nef and HIV-1 Vpu in overcoming restriction by tetherin/BST2. PLoS Pathog. **5:**e1000429.
27. **Jolly, C., K. Kashefi, M. Hollinshead, and Q. J. Sattentau.** 2004. HIV-1 cell to cell transfer across an Env-induced, actin-dependent synapse. J. Exp. Med. **199:**283–293.
28. **Jolly, C., I. Mitar, and Q. J. Sattentau.** 2007. Adhesion molecule interactions facilitate human immunodeficiency virus type 1-induced virological synapse formation between T cells. J. Virol. **81:**13916–13921.
29. **Jolly, C., I. Mitar, and Q. J. Sattentau.** 2007. Requirement for an intact T cell actin and tubulin cytoskeleton for efficient HIV-1 assembly and spread. J. Virol. **81:**5547–5560.
30. **Jolly, C., and Q. J. Sattentau.** 2005. Human immunodeficiency virus type 1 virological synapse formation in T cells requires lipid raft integrity. J. Virol. **79:**12088–12094.
31. **Jouvenet, N., S. J. Neil, M. Zhadina, T. Zang, Z. Kratovac, Y. Lee, M. McNatt, T. Hatziioannou, and P. D. Bieniasz.** 2009. Broad-spectrum inhibition of retroviral and filoviral particle release by tetherin. J. Virol. **83:**1837–1844.
32. **Kaiser, G., H. Jaeger, J. Birkmann, J. Poppinger, J. M. Cummins, and W. M. Gallmeier.** 1992. Low-dose oral natural human interferon-alpha in 29 patients with HIV-1 infection: a double-blind, randomized, placebo-controlled trial. AIDS **6:**563–569.
33. **Klimkait, T., K. Strebel, M. D. Hoggan, M. A. Martin, and J. M. Orenstein.** 1990. The human immunodeficiency virus type 1-specific protein vpu is required for efficient virus maturation and release. J. Virol. **64:**621–629.
34. **Kupzig, S., V. Korolchuk, R. Rollason, A. Sugden, A. Wilde, and G. Banting.** 2003. Bst-2/HM1.24 is a raft-associated apical membrane protein with an unusual topology. Traffic **4:**694–709.
35. **Landau, A., D. Batisse, C. Piketty, and M. D. Kazatchkine.** 2000. Effect of interferon and ribavirin on HIV viral load. AIDS **14:**96–97.
36. **Le Tortorec, A., and S. J. Neil.** 2009. Antagonism to and intracellular sequestration of human tetherin by the human immunodeficiency virus type 2 envelope glycoprotein. J. Virol. **83:**11966–11978.
37. **Maldarelli, F., M. Y. Chen, R. L. Willey, and K. Strebel.** 1993. Human immunodeficiency virus type 1 Vpu protein is an oligomeric type I integral membrane protein. J. Virol. **67:**5056–5061.
38. **Malim, M. H., and M. Emerman.** 2008. HIV-1 accessory proteins—ensuring viral survival in a hostile environment. Cell Host Microbe **3:**388–398.
39. **Mangeat, B., G. Gers-Huber, M. Lehmann, M. Zufferey, J. Luban, and V. Piguet.** 2009. HIV-1 Vpu neutralizes the antiviral factor tetherin/BST-2 by binding it and directing its beta-TrCP2-dependent degradation. PLoS Pathog. **5:**e1000574.
40. **Mansouri, M., K. Viswanathan, J. L. Douglas, J. Hines, J. Gustin, A. V. Moses, and K. Fruh.** 2009. Molecular mechanism of BST2/tetherin down-regulation by K5/MIR2 of Kaposi's sarcoma-associated herpesvirus. J. Virol. **83:**9672–9681.
41. **Martin, N., S. Welsch, C. Jolly, J. A. Briggs, D. Vaux, and Q. J. Sattentau.** 2010. Virological synapse-mediated spread of human immunodeficiency virus type 1 between T cells is sensitive to entry inhibition. J. Virol. **84:**3516–3527.
42. **McDonald, D., L. Wu, S. M. Bohks, V. N. KewalRamani, D. Unutmaz, and T. J. Hope.** 2003. Recruitment of HIV and its receptors to dendritic cell-T cell junctions. Science **300:**1295–1297.
43. **Mehandru, S., M. A. Poles, K. Tenner-Racz, A. Horowitz, A. Hurley, C. Hogan, D. Boden, P. Racz, and M. Markowitz.** 2004. Primary HIV-1 infection is associated with preferential depletion of CD4+ T lymphocytes from effector sites in the gastrointestinal tract. J. Exp. Med. **200:**761–770.
44. **Mitchell, R. S., C. Katsura, M. A. Skasko, K. Fitzpatrick, D. Lau, A. Ruiz, E. B. Stephens, F. Margottin-Goguet, R. Benarous, and J. C. Guatelli.** 2009. Vpu antagonizes BST-2-mediated restriction of HIV-1 release via beta-TrCP and endo-lysosomal trafficking. PLoS Pathog. **5:**e1000450.
45. **Miyagi, E., A. J. Andrew, S. Kao, and K. Strebel.** 2009. Vpu enhances HIV-1 virus release in the absence of Bst-2 cell surface down-modulation and intracellular depletion. Proc. Natl. Acad. Sci. U. S. A. **106:**2868–2873.
46. **Neil, S., and P. Bieniasz.** 2009. HIV, restriction factors, and interferon. J. Interferon Cytokine Res. **29:**569–580.
47. **Neil, S. J., S. W. Eastman, N. Jouvenet, and P. D. Bieniasz.** 2006. HIV-1 Vpu promotes release and prevents endocytosis of nascent retrovirus particles from the plasma membrane. PLoS Pathog. **2:**e39.
48. **Neil, S. J., V. Sandrin, W. I. Sundquist, and P. D. Bieniasz.** 2007. An

interferon-alpha-induced tethering mechanism inhibits HIV-1 and Ebola virus particle release but is counteracted by the HIV-1 Vpu protein. Cell Host Microbe **2:**193–203.
49. **Neil, S. J., T. Zang, and P. D. Bieniasz.** 2008. Tetherin inhibits retrovirus release and is antagonized by HIV-1 Vpu. Nature **451:**425–430.
50. **Nguyen, D., and J. Hildreth.** 2000. Evidence for budding of human immunodeficiency virus type 1 selectively from glycolipid-enriched membrane lipid rafts. J. Virol. **74:**3264–3272.
51. **Ono, A., and E. O. Freed.** 2001. Plasma membrane rafts play a critical role in HIV-1 assembly and release. Proc. Natl. Acad. Sci. U. S. A. **98:**13925–13930.
52. **Orholm, M., C. Pedersen, L. Mathiesen, P. Dowd, and J. O. Nielsen.** 1989. Suppression of p24 antigen in sera from HIV-infected individuals with low-dose alpha-interferon and zidovudine: a pilot study. AIDS **3:**97–100.
53. **Pais-Correia, A. M., M. Sachse, S. Guadagnini, V. Robbiati, R. Lasserre, A. Gessain, O. Gout, A. Alcover, and M. I. Thoulouze.** 2010. Biofilm-like extracellular viral assemblies mediate HTLV-1 cell-to-cell transmission at virological synapses. Nat. Med. **16:**83–89.
54. **Pardieu, C., R. Vigan, S. Wilson, A. Calvi, T. Zang, P. D. Bieniasz, P. Kellam, G. J. Towers, and S. J. D. Neil.** 2010. The RING-CH ligase K5 antagonizes restriction of KSHV and HIV-1 particle release by mediating ubituitin-dependent endosomal degradation of tetherin. PLoS Pathog. **15:**e1000843.
55. **Pearce-Pratt, R., D. Malamud, and D. M. Phillips.** 1994. Role of the cytoskeleton in cell-to-cell transmission of human immunodeficiency virus. J. Virol. **68:**2898–2905.
56. **Perez-Caballero, D., T. Zang, A. Ebrahimi, M. W. McNatt, D. A. Gregory, M. C. Johnson, and P. D. Bieniasz.** 2009. Tetherin inhibits HIV-1 release by directly tethering virions to cells. Cell **139:**499–511.
57. **Phillips, D.** 1994. The role of cell-to-cell transmission in HIV infection. AIDS **8:**719–731.
58. **Richardson, M. W., R. G. Carroll, M. Stremlau, N. Korokhov, L. M. Humeau, G. Silvestri, J. Sodroski, and J. L. Riley.** 2008. Mode of transmission affects the sensitivity of human immunodeficiency virus type 1 to restriction by rhesus TRIM5alpha. J. Virol. **82:**11117–11128.
59. **Rivero, J., M. Fraga, I. Cancio, J. Cuervo, and P. Lopez-Saura.** 1997. Long-term treatment with recombinant interferon alpha-2b prolongs survival of asymptomatic HIV-infected individuals. Biotherapy **10:**107–113.
60. **Rollason, R., V. Korolchuk, C. Hamilton, M. Jepson, and G. Banting.** 2009. A CD317/tetherin-RICH2 complex plays a critical role in the organization of the subapical actin cytoskeleton in polarized epithelial cells. J. Cell Biol. **184:**721–736.
61. **Rudnicka, D., J. Feldmann, F. Porrot, S. Wietgrefe, S. Guadagnini, M. C. Prevost, J. Estaquier, A. T. Haase, N. Sol-Foulon, and O. Schwartz.** 2009. Simultaneous cell-to-cell transmission of human immunodeficiency virus to multiple targets through polysynapses. J. Virol. **83:**6234–6246.
62. **Sakuma, T., T. Noda, S. Urata, Y. Kawaoka, and J. Yasuda.** 2009. Inhibition of Lassa and Marburg virus production by tetherin. J. Virol. **83:**2382–2385.
63. **Salazar-Gonzalez, J. F., M. G. Salazar, B. F. Keele, G. H. Learn, E. E. Giorgi, H. Li, J. M. Decker, S. Wang, J. Baalwa, M. H. Kraus, N. F. Parrish, K. S. Shaw, M. B. Guffey, K. J. Bar, K. L. Davis, C. Ochsenbauer-Jambor, J. C. Kappes, M. S. Saag, M. S. Cohen, J. Mulenga, C. A. Derdeyn, S. Allen, E. Hunter, M. Markowitz, P. Hraber, A. S. Perelson, T. Bhattacharya, B. F. Haynes, B. T. Korber, B. H. Hahn, and G. M. Shaw.** 2009. Genetic identity, biological phenotype, and evolutionary pathways of transmitted/founder viruses in acute and early HIV-1 infection. J. Exp. Med. **206:**1273–1289.
64. **Sato, H., J. Orenstein, D. Dimitrov, and M. Martin.** 1992. Cell-cell spread of HIV-1 occurs within minutes and may not involve the participation of virus particles. Virology **186:**712–724.
65. **Sattentau, Q.** 2008. Avoiding the void: cell-to-cell spread of human viruses. Nat. Rev. Microbiol. **6:**815–826.
66. **Sauter, D., M. Schindler, A. Specht, W. N. Landford, J. Munch, K. A. Kim, J. Votteler, U. Schubert, F. Bibollet-Ruche, B. F. Keele, J. Takehisa, Y. Ogando, C. Ochsenbauer, J. C. Kappes, A. Ayouba, M. Peeters, G. H. Learn, G. Shaw, P. M. Sharp, P. Bieniasz, B. H. Hahn, T. Hatziioannou, and F. Kirchhoff.** 2009. Tetherin-driven adaptation of Vpu and Nef function and the evolution of pandemic and nonpandemic HIV-1 strains. Cell Host Microbe **6:**409–421.
67. **Schacker, T., S. Little, E. Connick, K. Gebhard-Mitchell, Z.-Q. Zhang, J. Krieger, J. Pryor, D. Havlir, J. Wong, D. Richman, L. Corey, and A. Haase.** 2000. Rapid accumulation of human immunodeficiency virus (HIV) in lymphatic tissue reservoirs during acute and early HIV infection: implications for timing of antiretroviral therapy. J. Infect. Dis. **181:**354–357.
68. **Schubert, U., K. A. Clouse, and K. Strebel.** 1995. Augmentation of virus secretion by the human immunodeficiency virus type 1 Vpu protein is cell type independent and occurs in cultured human primary macrophages and lymphocytes. J. Virol. **69:**7699–7711.
69. **Sheehy, A. M., N. C. Gaddis, J. D. Choi, and M. H. Malim.** 2002. Isolation of a human gene that inhibits HIV-1 infection and is suppressed by the viral Vif protein. Nature **418:**646–650.
70. **Sherer, N. M., J. Jin, and W. Mothes.** 2010. Directional spread of surface-associated retroviruses regulated by differential virus-cell interactions. J. Virol. **84:**3248–3258.
71. **Sherer, N. M., M. J. Lehmann, L. F. Jimenez-Soto, C. Horensavitz, M. Pypaert, and W. Mothes.** 2007. Retroviruses can establish filopodial bridges for efficient cell-to-cell transmission. Nat. Cell Biol. **9:**310–315.
72. **Skillman, D. R., J. L. Malone, C. F. Decker, K. F. Wagner, R. L. Mapou, M. J. Liao, D. Testa, and M. S. Meltzer.** 1996. Phase I trial of interferon alfa-n3 in early-stage human immunodeficiency virus type 1 disease: evidence for drug safety, tolerance, and antiviral activity. J. Infect. Dis. **173:**1107–1114.
73. **Sol-Foulon, N., M. Sourisseau, F. Porrot, M. I. Thoulouze, C. Trouillet, C. Nobile, F. Blanchet, V. di Bartolo, N. Noraz, N. Taylor, A. Alcover, C. Hivroz, and O. Schwartz.** 2007. ZAP-70 kinase regulates HIV cell-to-cell spread and virological synapse formation. EMBO J. **26:**516–526.
74. **Sourisseau, M., N. Sol-Foulon, F. Porrot, F. Blanchet, and O. Schwartz.** 2007. Inefficient human immunodeficiency virus replication in mobile lymphocytes. J. Virol. **81:**1000–1012.
75. **Sowinski, S., C. Jolly, O. Berninghausen, M. A. Purbhoo, A. Chauveau, K. Kohler, S. Oddos, P. Eissmann, F. M. Brodsky, C. Hopkins, B. Onfelt, Q. Sattentau, and D. M. Davis.** 2008. Membrane nanotubes physically connect T cells over long distances presenting a novel route for HIV-1 transmission. Nat. Cell Biol. **10:**211–219.
76. **Sperber, S. J., D. J. Gocke, C. A. Haberzettl, and S. Pestka.** 1993. Low-dose oral recombinant interferon-alpha A in patients with HIV-1 infection: a blinded pilot study. AIDS **7:**693–697.
77. **Strebel, K., T. Klimkait, F. Maldarelli, and M. A. Martin.** 1989. Molecular and biochemical analyses of human immunodeficiency virus type 1 vpu protein. J. Virol. **63:**3784–3791.
78. **Strebel, K., T. Klimkait, and M. A. Martin.** 1988. A novel gene of HIV-1, vpu, and its 16-kilodalton product. Science **241:**1221–1223.
79. **Stremlau, M., C. M. Owens, M. J. Perron, M. Kiessling, P. Autissier, and J. Sodroski.** 2004. The cytoplasmic body component TRIM5alpha restricts HIV-1 infection in Old World monkeys. Nature **427:**848–853.
80. **Terwilliger, E. F., E. A. Cohen, Y. C. Lu, J. G. Sodroski, and W. A. Haseltine.** 1989. Functional role of human immunodeficiency virus type 1 vpu. Proc. Natl. Acad. Sci. U. S. A. **86:**5163–5167.
81. **Van Damme, N., D. Goff, C. Katsura, R. L. Jorgenson, R. Mitchell, M. C. Johnson, E. B. Stephens, and J. Guatelli.** 2008. The interferon-induced protein BST-2 restricts HIV-1 release and is downregulated from the cell surface by the viral Vpu protein. Cell Host Microbe **3:**245–252.
82. **Varthakavi, V., R. M. Smith, S. P. Bour, K. Strebel, and P. Spearman.** 2003. Viral protein U counteracts a human host cell restriction that inhibits HIV-1 particle production. Proc. Natl. Acad. Sci. U. S. A. **100:**15154–15159.
83. **Veazey, R. S., M. DeMaria, L. V. Chalifoux, D. E. Shvetz, D. R. Pauley, H. L. Knight, M. Rosenzweig, R. P. Johnson, R. C. Desrosiers, and A. A. Lackner.** 1998. Gastrointestinal tract as a major site of CD4+ T cell depletion and viral replication in SIV infection. Science **280:**427–431.
84. **Vendrame, D., M. Sourisseau, V. Perrin, O. Schwartz, and F. Mammano.** 2009. Partial inhibition of human immunodeficiency virus replication by type I interferons: impact of cell-to-cell viral transfer. J. Virol. **83:**10527–10537.
85. **Yao, X. J., S. Garzon, F. Boisvert, W. A. Haseltine, and E. A. Cohen.** 1993. The effect of vpu on HIV-1-induced syncytia formation. J. Acquir. Immune Defic. Syndr. **6:**135–141.
86. **Zhang, F., S. J. Wilson, W. C. Landford, B. Virgen, D. Gregory, M. C. Johnson, J. Munch, F. Kirchhoff, P. D. Bieniasz, and T. Hatziioannou.** 2009. Nef proteins from simian immunodeficiency viruses are tetherin antagonists. Cell Host Microbe **6:**54–67.